Zoological Journal of the Linnean Society, 2023, **197**, 719–751. With 15 figures.

Revealing the cryptic diversity of the widespread and poorly known South American blind snake genus *Amerotyphlops* (Typhlopidae: Scolecophidia) through integrative taxonomy

ROBERTA GRABOSKI[1–3,*], JUAN C. ARREDONDO[4], FELIPE G. GRAZZIOTIN[5], RICARDO ARTURO GUERRA-FUENTES[3,6], ARIANE A. A. DA SILVA[7], ANA L. C. PRUDENTE[3], ROBERTA R. PINTO[8], MIGUEL T. RODRIGUES[9], SANDRO L. BONATTO[10] and HUSSAM ZAHER[1]

[1]*Museu de Zoologia da Universidade de São Paulo, Avenida Nazaré, Caixa Postal 42494, CEP 04218-070, São Paulo, São Paulo, Brazil*
[2]*Programa de Pós-Graduação em Zoologia, Universidade Estadual Paulista Júlio de Mesquita Filho, Avenida 24 A, Bela Vista, CEP 13506-900, Rio Claro, São Paulo, Brazil*
[3]*Laboratório de Herpetologia, Coordenação de Zoologia, Museu Paraense Emílio Goeldi, Avenida Perimetral, Terra Firme, Caixa Postal 399, CEP 66077-530, Belém, Pará, Brazil*
[4]*Colecciones Biológicas de la Universidad CES (CBUCES), Facultad de Ciencias y Biotecnología, Universidad CES, Calle 10A, Medellín, Colombia*
[5]*Laboratório de Coleções Zoológicas, Instituto Butantan, Avenida Vital Brasil, Butantã, São Paulo - SP, 05503-900, Brazil*
[6]*Faculdade de Ciências Naturais, Campus Universitário do Tocantins-Cametá, Universidade Federal do Pará, Travessa Padre Antônio Franco, 2617, Bairro da Matinha, CEP 68400-000 Cametá, Pará, Brazil*
[7]*Instituto Nacional de Pesquisas da Amazônia, Programa de Coleções e Acervos Científicos, Avenida André de Araújo, CEP 69060-000, Manaus, Amazonas, Brazil*
[8]*Laboratório de Diversidade de Anfíbios e Répteis, Museu de Arqueologia e Ciências Naturais da Universidade Católica de Pernambuco, Universidade Católica de Pernambuco, Recife, Brazil*
[9]*Universidade de São Paulo, Instituto de Biociências, Departamento de Zoologia, Caixa Postal 11.461, CEP 05508-090, São Paulo, SP, Brazil*
[10]*Laboratório de Biologia Genômica e Molecular, Escola de Ciências da Saúde e da Vida, Pontifícia Universidade Católica do Rio Grande do Sul, Avenida Ipiranga, CEP 90619-900, Porto Alegre, Rio Grande do Sul, Brazil*

Received 22 June 2021; revised 20 June 2022; accepted for publication 1 July 2022

Morphological stasis is generally associated with relative constancy in ecological pressures throughout time, producing strong stabilizing selection that retains similar shared morphology. Although climate and vegetation are commonly the main key factors driving diversity and phenotypic diversification in terrestrial vertebrates, fossorial organisms have their morphology mostly defined by their fossorial lifestyle. Among these secretive fossorial organisms, blind snakes of the South American genus *Amerotyphlops* are considered poorly studied when compared to other taxa. Here, we evaluate the cryptic diversity of *Amerotyphlops* using phylogenetic and multivariate approaches. We based our phylogenetic analysis on a molecular dataset composed of 12 gene fragments (eight nuclear and four mitochondrial) for 109 species of Typhlopidae. The multivariate analysis was implemented using 36 morphological variables for

*Corresponding author. E-mail: roberta.graboski@gmail.com
[Version of record, published online 12 November 2022; http://zoobank.org/ urn:lsid:zoobank.org:pub:9E6031A3-0186-415B-86D3-24F6F267DD10]

377 specimens of *Amerotyphlops*. Additionally, we contrast our phylogenetic result with the morphological variation found in cranial, external and hemipenial traits. Our phylogenetic results recovered with strong support the following monophyletic groups within *Amerotyphlops*: (1) a clade formed by *A. tasymicris* and *A. minuisquamus*; (2) a clade composed of *A. reticulatus*; (3) a north-eastern Brazilian clade including *A. yonenagae*, *A. arenensis*, *A. paucisquamus* and *A. amoipira*; and (4) a clade composed of *A. brongersmianus* and a complex of cryptic species. Based on these results we describe four new species of *Amerotyphlops* from north-eastern and south-eastern Brazil, which can be distinguished from the morphologically similar species, *A. brongersmianus* and *A. arenensis*.

ADDITIONAL KEYWORDS: Atlantic Rain Forest – new species – phylogenetics – Serpentes.

INTRODUCTION

In the last two decades, cryptic species have posed a challenge for biologists and taxonomists (Winker, 2005). Cryptic species are considered morphologically indistinguishable evolutionary units, which are usually classified as a single species, even when other evidence indicates that they have unique evolutionary trajectories (Bickford *et al.*, 2007; Fišer *et al.*, 2018; Struck *et al.*, 2018; Struck & Cerca, 2019). Despite distinct evolutionary trajectories, usually the phenotypes of cryptic species are driven by equalizing evolutionary forces causing morphological stasis, convergence, parallelism and phylogenetic niche conservatism (Bickford *et al.*, 2007; Fišer *et al.*, 2018; Struck *et al.*, 2018). Among these evolutionary forces, morphological stasis can be properly tested through molecular phylogenetic analysis (Bickford *et al.*, 2007). Groups of cryptic species under morphological stasis, although retaining a high degree of phenotypic similarity, usually present deep phylogenetic structure (Struck *et al.*, 2018; Struck & Cerca, 2019). Stasis is generally associated with relative constancy in ecological pressures throughout time, producing strong stabilizing selection that retains a similar shared morphology (Swift *et al.*, 2016; Struck *et al.*, 2018; Struck & Cerca, 2019).

Although climate and vegetation are commonly the main key factors driving diversity and phenotypic diversification in terrestrial vertebrates (Stayton, 2005), fossorial organisms have their morphology mostly defined by their burrowing lifestyle and the characteristics of the soils in which they burrow (Daly & Patton, 1990; Reig *et al.*, 1990; Steinberg *et al.*, 2000; Massarini *et al.*, 2002; Mulvaney *et al.*, 2005; Daniels *et al.*, 2009; Parham & Papenfuss, 2009; Marcy *et al.*, 2016).

Vertebrates with a fossorial and subterranean lifestyle are difficult to obtain and observe due to their secretive behaviours, and many aspects of their evolutionary biology remain poorly known, resulting in an underestimation of their diversity (Massarini *et al.*, 2002; Fernández-Stolz *et al.*, 2007; Thomas & Hedges, 2007; Gonçalves & de Freitas, 2009; Correia *et al.*, 2018; Maddock *et al.*, 2020; O'Connell *et al.*, 2021). Among these secretive subterranean organisms, Scolecophidia (Typhlopoidea, Leptotyphlopidae and Anomalepididae) represents one of the most understudied groups. Despite recent advances in higher level systematics of scolecophidians (Adalsteinsson *et al.*, 2009; Hedges *et al.*, 2014; Pyron & Wallach, 2014; Graboski *et al.*, 2018), the diversity in the species-rich South American radiation has not been explored so far through integrative approaches.

Amerotyphlops Hedges *et al.* (2014) was proposed for a clade of Neotropical typhlopids that currently comprises 15 species, 14 of which are distributed on the continent, from Mexico to northern Argentina, and one occurring in the West Indies (Hedges *et al.*, 2014; Pyron & Wallach, 2014). Of the 14 mainland species, eight are restricted to South America (see the Supporting Information, Table S1 for detailed distribution): (1) *Amerotyphlops reticulatus* (Linnaeus, 1758), (2) *A. lehneri* (Roux, 1926), (3) *A. brongersmianus* (Vanzolini, 1972, 1976), (4) *A. minuisquamus* (Dixon & Hendricks, 1979), (5) *A. paucisquamus* (Dixon & Hendricks, 1979), (6) *A. yonenagae* (Rodrigues, 1991), (7) *A. amoipira* (Rodrigues & Juncá, 2002) and (8) *A. arenensis* (Graboski *et al.*, 2015). Despite the wide geographic distribution of South American blind snakes, they are often poorly sampled in phylogenetic studies, due to their secretive habits and the lack of comprehensive taxonomic studies.

Here, we evaluate the genetic and morphological diversity of *Amerotyphlops*, aiming to test the existence of cryptic species in the genus. Our results provide evidence of the existence of four new species from north-eastern and south-eastern Brazil that can be distinguished from the morphologically similar species, *A. brongersmianus* and *A. arenensis*.

MATERIAL AND METHODS

TAXON AND GENE SAMPLING

Our data matrix comprises 149 terminals (including 109 described species) sequenced for 12 genes: four mitochondrial (12S, 16S, *cytb* and *cox1*) and eight nuclear (*bdnf*, *rag1*, *bmp2*, *nt3*, *prlr*, *jun*, *dnh3* and *amel*). We sequenced 124 new DNA fragments (GenBank accession numbers: OP093574–OP093604; OP094006–OP094029; OP177794–OP177861) for seven described species of *Amerotyphlops* (*A. arenensis*, *A. amoipira*, *A. brongersmianus*, *A. minuisquamus*,

A. paucisquamus, *A. reticulatus* and *A. yonenagae*) and four new species described in this study (Supporting Information, Table S2).

We also included sequences from GenBank for four subfamilies of Typhlopidae: Afrotyphlopinae (19 species), Asiatyphlopinae (43 species), Madatyphlopinae (six species) and Typhlopinae (39 species) (Supporting Information, Table S3). Additionally, we also included sequences for four other families of scolecophidians: Anomalepididae [*Liotyphlops albirostris* (Peters, 1858)], Leptotyphlopidae [*Epictia columbi* (Klauber, 1939) and *Rena dulcis* Baird & Girard, 1853], Gerrhopilidae [*Gerrhopilus mirus* (Jan, 1860) and *Gerrhopilus hedraeus* (Savage, 1950)] and Xenotyphlopidae [*Xenotyphlops grandidieri* (Mocquard, 1905)] (Supporting Information, Table S3). All sequences of scolecophidians from GenBank included in our analysis were mainly generated by the following previous taxonomic studies: Vidal *et al.* (2010), Hedges *et al.* (2014), Marin *et al.* (2013a, b) and Graboski *et al.* (2018) (see Supporting Information, Table S3 for accession numbers). We rooted our phylogenetic tree with Anomalepididae and Leptotyphlopidae.

DNA sequencing

DNA was extracted following the protocol described by Hillis *et al.* (1996). Sequences were amplified via polymerase chain reaction (PCR) using the primers for: 12S and 16S, as described by Zaher *et al.* (2009); *cytb*, as described by Grazziotin *et al.* (2012); *bdnf* and *cox1*, as described by Graboski *et al.* (2018); *jun*, as described by Zaher *et al.* (2009); and *dnh3*, as described by Townsend *et al.* (2008).

PCRs were performed using standard protocols, with adjustments to increase the efficiency of amplification, as following: the addition of 10% of Trehalose for 12S, 16S, *cytb* and *cox1*, or 0.4% of Triton 100 for *bdnf*, *dnh3* and *jun*. We used the annealing temperature of 54 °C for 12S and 16S; 56 °C *for bdnf*, *jun* and *dnh3*; and a touch-down cycle of 60–50 °C with final annealing of 54 °C for *cytb* and *cox1*. Amplified fragments were purified with shrimp alkaline phosphatase and exonuclease I (GE healthcare, Piscataway, NJ) and both strands were processed using the DYEnamic ET Dye Terminator Cycle Sequencing Kit in a MegaBACE 1000 automated sequencer (GE healthcare), following the manufacturer's protocols. Both strands were quality checked and, when necessary, manually edited. The consensus of both strands was generated using Geneious Prime® 2022.1.1 (https://www.geneious.com, Kearse *et al.*, 2012).

Molecular analyses

Sequences were aligned using MAFFT v.1.3.6 (Katoh & Standley, 2013) as implemented in Geneious Prime (see our concatenated alignment in the Supporting Information, Appendix S1). The 12S and 16S were aligned under the E-INS-i algorithm, while *cox1*, *cytb*, and the nuclear genes were aligned under the G-INS-i algorithm. We used default parameters for gap opening and extension. All protein-coding genes were visually checked using Geneious Prime to verify if all sequences follow the correct reading frame.

We used PartitionFinder 2 (Lanfear *et al.*, 2016) to identify the combined sets of partitioning schemes and models of molecular evolution. We divided our matrix into 32 partitions (coding genes were partitioned by codon positions and each rRNA was analysed as a separate partition) and performed a search using the greedy option. We used the Akaike information criterion with correction (AICc) to select the best fit model of evolution. We only allowed the selection of models implemented in RAxML (i.e., GTR and GTR+GAMMA). To avoid overcorrection regarding values of alpha and P-Invar (proportion of invariant sites), we did not allow PartitionFinder to select models with P-Invar, as suggested in the RAxML manual.

We performed a maximum likelihood (ML) analysis using RAxML v.8.2.3 (Stamatakis, 2014). The ML tree was estimated using the RAxML algorithm that conducts a rapid bootstrap analysis and searches for best-scoring ML tree in the same run (option *-f a*). We ran 1000 bootstrap replicates, and the best-scoring ML tree was estimated 200 times using as starting tree each fifth bootstrap tree. Additionally, we calculated the patristic distance among Typhlopinae (*Amerotyphlops*, *Antillotyphlops* Hedges *et al.*, 2014, *Cubatyphlops* Hedges *et al.*, 2014 and *Typhlops* Oppel, 1811) using the R package *ape* (Paradis & Schliep, 2019)

Specimens and characters examined for morphological analysis

We examined a total of 377 specimens (347 specimens for pholidosis; 176 specimens for morphometrics) representing all mainland South American species of *Amerotyphlops* (Supporting Information, Appendices S2, S3). To correctly identify all examined specimens, we used the available information in the literature, as previous taxonomic revisions (Dixon & Hendricks, 1979; Graboski *et al.*, 2018), the information available in the original description (Linnaeus, 1758; Vanzolini, 1972, 1976; Dixon & Hendricks, 1979; Rodrigues, 1991; Rodrigues & Juncá, 2002; Graboski *et al.*, 2015) and by reviewing the type series of species (see Supporting Information, Appendices S2, S3). Additionally, for Central America congeneric species (i.e. *Amerotyphlops costaricensis* (Jiménez & Savage, 1962), *A. lehneri* (Roze, 1956), *A. microstomus* (Cope, 1866), *A. stadelmani* (Schmidt, 1936), *A. tasymicris* (Thomas, 1974), *A. tenuis* (Salvin, 1860), *A. trinitatus*

(Richmond, 1965) and *A. tycherus* (Townsend *et al.*, 2008) we used the information available in the original description and previous taxonomic revisions.

We used our phylogenetic tree as a framework to evaluate both external and internal morphology (hemipenis and skull), searching for diagnostic characters for the retrieved phylogenetic lineages. We measured the total length (TTL) and snout–vent length (SVL) to the nearest 1 mm by carefully stretching the specimen along a graduated ruler, and for other measurements we used a digital calliper to the nearest 0.1 mm. Our definitions of external morphological characters followed Dixon & Hendricks (1979) and Thomas & Hedges (2007) or were defined in the present study. We examined a total of 41 characters from external morphology: 12 categorical, 15 continuous and 14 ratios between continuous variables. In the descriptions, a slash (/) is used for rows counts from the anterior/median/posterior part of the body (Supporting Information, Table S4). We determined the sex of the individuals by making a small incision at the base of the tail to assess the presence (male) or absence (female) of hemipenes.

We examined four hemipenes of the candidate species *Amerotyphlops* sp. 2 from South America (see Supporting Information, Appendix S2). We everted hemipenes from fresh specimens or, alternatively, from fixed specimens following the protocols described by Zaher (1999) and Zaher & Prudente (2003). Hemipenial terminology follows Branch (1986), Peters & Orejas-Miranda (1970), Graboski *et al.* (2018) and Montingelli et al. (2022). We photographed the hemipenes using a Leica DFC425 digital camera attached to a Leica M205a stereoscopic microscope and made the combination and montage of multifocal photographs using the Leica Application Suite software (LAS core v.3.8, Leica Microsystems).

All specimens examined (Supporting Information, Appendices S2, S3) are deposited in the following institutions in Brazil (acronyms in parentheses): Laboratório de Anfíbios e Répteis, Universidade Federal do Rio Grande do Norte, Natal, Rio Grande do Norte, under the care of Adrian Antônio Garda (AAGARDA); Laboratório de Herpetologia do Instituto de Biociências, Universidade de São Paulo, São Paulo, under the care of Miguel Trefaut Rodrigues (MTR) and Gindomar Gomes Santana (GGS). Other museum acronyms follow Sabaj (2019) and Frost (2018).

Maps of species distribution

We also built a geographical dataset of 456 distribution records for the species of *Amerotyphlops* that have sympatric distribution with the new species described here (i.e. *A. amoipira*, *A. arenensis*, *A. brongersmianus*, *A. paucisquamus* and *A. yonenagae*). Maps were generated through the software ArcGIS v.10.2.2 (ESRI 1999). Initially, we obtained the geographical coordinates from the Species Link online database (https://splink.cria.org.br), which is based on institutions' databases. We evaluated these registers through the contrast with our current knowledge about the group, and we included additional localities compiled from the literature – previous taxonomic revisions, information available in the original description and lists of species distribution (Dixon & Hendricks, 1979; Rodrigues, 1991; Rodrigues & Juncá, 2002; Van-Silva *et al.*, 2007; Santana *et al.*, 2008; Martins *et al.*, 2010; de Arruda *et al.*, 2011; Caicedo-Portilla, 2011; de Brito & Freire, 2012; de França *et al.*, 2012; Guedes *et al.*, 2014; Wallach *et al.*, 2014; Graboski *et al.*, 2015, 2018; Roberto *et al.*, 2015, 2017; de Freitas *et al.*, 2019; Nogueira *et al.*, 2019). Additionally, we included in the geographical dataset registers taken directly from the localities of specimens examined in collections (see Supporting Information, Appendices S2, S3)

High-resolution X-ray computed tomography and osteological comparisons of cranial anatomy

We obtained data from skulls by using non-destructive high-resolution X-ray computed tomography (HRXCT) from seven specimens of the genus *Amerotyphlops* from South America (see Supporting Information, Appendix 2). All HRXCT data were generated using a GE phoenix v|tome|x m system at the Museu de Zoologia da Universidade de São Paulo, São Paulo, Brazil. The raw data were imported to VG STUDIO Max 2.1 and exported for analysis, segmentation and visualization. We segmented each bone slide by slide by considering the different densities of bones, applying threshold tools. We isolated or removed cranial (lower jaws and quadrate) and postcranial elements, and the final volume was converted into an isosurface with triangular mesh (*.ply* files) in VG STUDIO Max. The segmentation was performed at the Museu de Zoologia da Universidade de São Paulo. Our cranial descriptions and comparisons followed the terminology employed by List (1966), Cundall & Irish (2008), Chretien *et al.* (2019) and Lira & Martins (2021). We measured the skull length (SL) from the posterior margin of the otoccipital to the mid-dorsal region of the premaxilla; the skull width (SW) between the frontal processes of the parietal; the length of the ventral portion of the pterygoid process of the palatine (VPPL) from the base of the process to its distal end; and the palatine foramen diameter (PFD) measuring the larger distance between two opposite point at the internal margin of the foramen. We measured all morphometric osteological

characters (Supporting Information, Table S5) to the nearest 0.01 mm directly on to the *.ply* files with the measurement tool implemented in the open source system MeshLab v.2020.06 (Cignoni *et al.*, 2008).

Meristic and morphometric comparisons

To test the existence of cryptic species using morphological evidence, we defined nine OTUs (operational taxonomic units) for South American diversity of *Amerotyphlops*. We based the definition of OTUs on previously described species and on the lineages recovered in our molecular phylogenetic analysis, as follows: OTU 1, *A. arenensis*; OTU 2, *A. yonenagae*; OTU 3, *A. amoipira*; OTU 4, *A. paucisquamus*; OTU 5, *A.* sp. 1, from Parque Nacional da Chapada Diamantina, on BR 144 Road, municipality Lençóis, Bahia state; OTU 6, *A.* sp. 2, from the Parque Nacional Serra das Lontras, municipality of Arataca, state of Bahia; OTU 7, *A.* sp. 3, from the Praia das Neves, municipality of Presidente Kennedy, state of Espírito Santo; and OTU 8, *A.* sp. 4, from municipality of Trancoso, state of Bahia; and OTU 9, *A. brongersmianus*.

Exploratory descriptive analysis was performed to summarize the character variations and to evaluate outliers through visual inspection of histograms and boxplots (see Supporting Information, Appendix S4) using the software R v.3.6.3 (R Core Team, 2017). We calculated mean, standard deviations and ranges (maximums and minimums) of the variables for all taxa and sexes. Normality was investigated through visual inspection of quantile–quantile plots (which also helps in the identification of outliers) and through Kolmogorov–Smirnov using *nortest* R package (Gross & Ligges, 2015). The homoscedasticity assumptions were tested through Levene using *car* R package (Fox & Weisberg, 2019). Sexual dimorphism was evaluated for all characters through *t*-tests with Bonferroni P-corrections (for normally distributed data) and a Wilcoxon test (for non-normally distributed data) within each species using 't.test' and 'wilcox.test' functions implemented in R package *stats* (R Core Team, 2017).

For an exploratory multivariate analysis, we created a new pipeline based on the R script used by Barbo *et al.* (2022b). We implemented the following three different approaches: (1) principal component analysis (PCA) based on our original dataset; (2) partial least square discriminant analysis (PLS-DA); and (3) linear discriminant analysis (LDA) based on a simulated equalized dataset. Because the sample size for some OTUs was not sufficient to perform PLS-DA and LDA, we implemented a pipeline to simulate an equalized dataset with 100 individuals per OTUs, regarding the original sample size for each OTU.

The pipeline to generate the simulated dataset was guided by the following rules: values for discrete and categorical variables for each OTU were drawn from (1) their binomial distribution – when only two 'states' were present for the variable – with a probability equal to the proportion of the OTUs more frequent state; or (2) from its Poisson distribution – when more than two 'states' were present – with a lambda equal to the OTUs median. Values from continuous variables were drawn from (3) their normal distribution with mean equal to the OTU's mean and standard deviation (SD) equal to the OTU's SD. When the OTU was represented by only one sample in the original dataset the values were draw from (4) the binomial distributions set to a probability of 0.95; (5) the Poisson distribution with lambda set as equal to the OTUs variable value; and (6) the normal distribution with mean set as equal to the OTUs variable value and the SD set as equal to the global SD (considering all OTUs).

The PCA was implemented based on the complete dataset, while the PLS-DA only used discrete characters and ratios, and the LDA was based only on the continuous characters. The LDA and PLS-DA analyses were performed in *MASS* (Vanables & Ripley, 2002) and *caret* (Kuhn, 2008) R packages, respectively. The dataset was scaled before implementing the PCA (correlation PCA), and before analysing the data in LDA, we removed variables presenting values of collinearity greater than 0.7. The training metric for PLS-DA was set to 'Accuracy' and scaled predictors were pre-processed by centring and scaling. The repeated cross-validation method was applied, and the training dataset was defined using three repeated ten-fold cross-validations to render a total of 30 accuracy estimation. We applied the 'one standard error' rule to select the optimal least complex model. The multivariate results were plotted using the R packages *ggplot2* (Wickham, 2016) and *ggbiplot* (Vu, 2011). All R scripts used in these analyses are available on Figshare (https://doi.org/10.6084/m9.figshare.20092721).

Species delimitation

Our understanding of species is based on the general lineage concept (i.e. species with separately evolving metapopulation lineages; de Queiroz, 2005), and we accessed the distinct evolutionary history of lineages of *Amerotyphlops* based on the analyses of genotypic and phenotypic diversity. Additionally, based on the evaluated morphological variation and the results of the statistical analyses, we considered populations as representing a new diagnosable species when they present a 'unique combination of characters states' (*sensu* Davis & Nixon, 1992).

RESULTS

PHYLOGENETIC ANALYSIS

Our concatenated alignment totalized 9107 base pairs (957 bp for 12S, 1414 bp for 16S, 1134 bp for *cytb*, 1205 bp for *cox1*, 709 bp for *bdnf*, 525 bp for *rag1*, 594 bp for *bmp2*, 639 bp for *nt3*, 486 bp for *prlr*, 378 bp for *amel*, 739 bp for *dnh3* and 327 bp for *jun*). The proportion of gaps and undetermined characters in the concatenated alignment was 65.3%. PARTITIONFINDER selected a scheme of partitions composed of 20 partitions with GTR+G and GTR models for the ML analysis (Supporting Information, Table S6).

The resulting ML topology (Fig. 1; Supporting Information, Fig. S1) for higher level affinities was similar to those presented by Vidal *et al.* (2010), Hedges *et al.* (2014), Pyron & Wallach (2014), Nagy *et al.* (2015), and Graboski *et al.* (2018). American typhlopids were recovered as a well-supported clade (95%) (Fig. 1; Supporting Information, Fig. S1) with two main clades within typhlopines. The first clade was formed by species from the Greater Antillean radiation (100%), and the second by species from South America and the Lesser Antilles (92%). In the latter clade, we found four well-supported monophyletic groups, as follows: (1) a clade formed by *A. tasymicris* and *A. minuisquamus* (75%); (2) a clade composed of *A. reticulatus* as the sister-group all the other South American species (87%); (3) a clade containing the north-eastern Brazilian species *A. arenensis*, *A. yonenagae*, *A. amoipira* and *A. paucisquamus* (clade A; 99%); and (4) a clade composed of the *A. brongersmianus* species complex (clade B; 87%).

Within clade B, we recovered five subclades: (1) a clade composed of one individual from the municipality of Lençóis, Bahia state, Brazil (*A.* sp. 1); (2) a clade composed of two individuals from Parque Nacional Serra das Lontras and Reserva Particular do Patrimônio Natural Serra do Teimoso, municipalities of Arataca and Jussari, respectively, in Bahia state, Brazil (*A.* sp. 2); (3) a clade composed of two individuals from Praia das Neves, Presidente Kennedy municipality, Espírito Santo state, Brazil (*A.* sp. 3); (4) a clade composed of one individual from the municipality of Trancoso, Bahia state, Brazil (*A.* sp. 4); and (5) a clade representing the species *Amerotyphlops brongersmianus*.

Patristic distances among species in the genera of Typhlopinae indicate a mean value of 0.13 considering all genera (standard deviation of 0.06). The genus *Amerotyphlops* shows the highest mean (0.19), while *Cubatyphlops* has the lowest mean (0.05). Patristic distances between the species of *Cubatyphlops* range from 0.014 to 0.96, with the lowest distance shown between *C. contorhinus* (Thomas & Hedges, 2007) and *C. notorachius* (Thomas & Hedges, 2007), and the highest distance between *C. biminiensis* (Richmond, 1955) and *C. caymanensis* (Sackett, 1940) (Supporting Information, Table S7). Patristic distances within *Antillotyphlops* range from 0.017 to 0.182, being the lowest distance between *A. naugus* (Thomas, 1966) and *A. richardi* (Duméril & Bibron, 1844), and the highest between *A. guadeloupensis* (Richmond, 1966) and *A. naugus* (Supporting Information, Table S8). Patristic distances within *Typhlops* range from 0.019 to 0.181, being the lowest distance between *T. hectus* Thomas, 1974 and *T. sylleptor* Thomas & Hedges, 2007, and the highest between *T. proancylops* Thomas & Hedges, 2007 and *T. pusillus* Barbour, 1914 (Supporting Information, Table S9).

Patristic distances among South American species range from 0.048 to 0.289, with the lowest distance being between *Amerotyphlops brongersmianus* and *A.* sp. 4, while the highest one was between *A. minuisquamus* and two species (*A. paucisquamus* and *A.* sp. 4). The genetic distance between *A. brongersmianus* and the four phylogenetically related clades (*A.* sp. 1, *A.* sp. 2, *A.* sp. 3 and *A.* sp. 4) ranges from 4% to 11.6% of divergence (Supporting Information, Table S10).

MORPHOLOGICAL ANALYSIS

Our exploratory analysis found a highly homogeneous pattern of cephalic scales for the genus *Amerotyphlops* throughout its geographic distribution. Thus, these characters were not informative for determining our OTUs as potential evolutionary units. The most useful morphological characters were the number of scales along the body (mid-dorsal, ventral and dorsal rows) and the measures and proportions of body traits (see Supporting Information, Appendix S4).

In the principal component analysis using 36 variables (discrete, continuous and ratios), based on the raw dataset, the first two components explained 35% (20% and 15%, respectively) of the total variance for males and females (Fig. 2A, B). The results obtained by PCA recognized two higher groups based on external morphology (Fig. 2A, B). The first group (GR1) is easily distinguished by having 18/18/18 dorsal row scales around the body, which correspond to species distributed exclusively in north-eastern Brazil, as follows: *A. arenensis*, *A. yonenagae*, *A. amoipira*, *A. paucisquamus* and *A.* sp. 1. The second group (GR2) is distinguished by having 20/20/20 or 20/20/18 dorsal row scales around the body, which correspond to OTUs distributed in north-eastern Brazil (*A.* sp. 2 and *A.* sp. 4), south-eastern Brazil (*A.* sp. 3) and the broadly distributed species *A. brongersmianus*.

In the PCA based on the simulated dataset, the first two components explained 34% (18% and 16%, respectively) and 35% (20% and 15%, respectively) of the total variance for GR1 and GR2, respectively (Supporting Information, Fig. S2A, B). The results obtained by PCA based on both raw and simulated

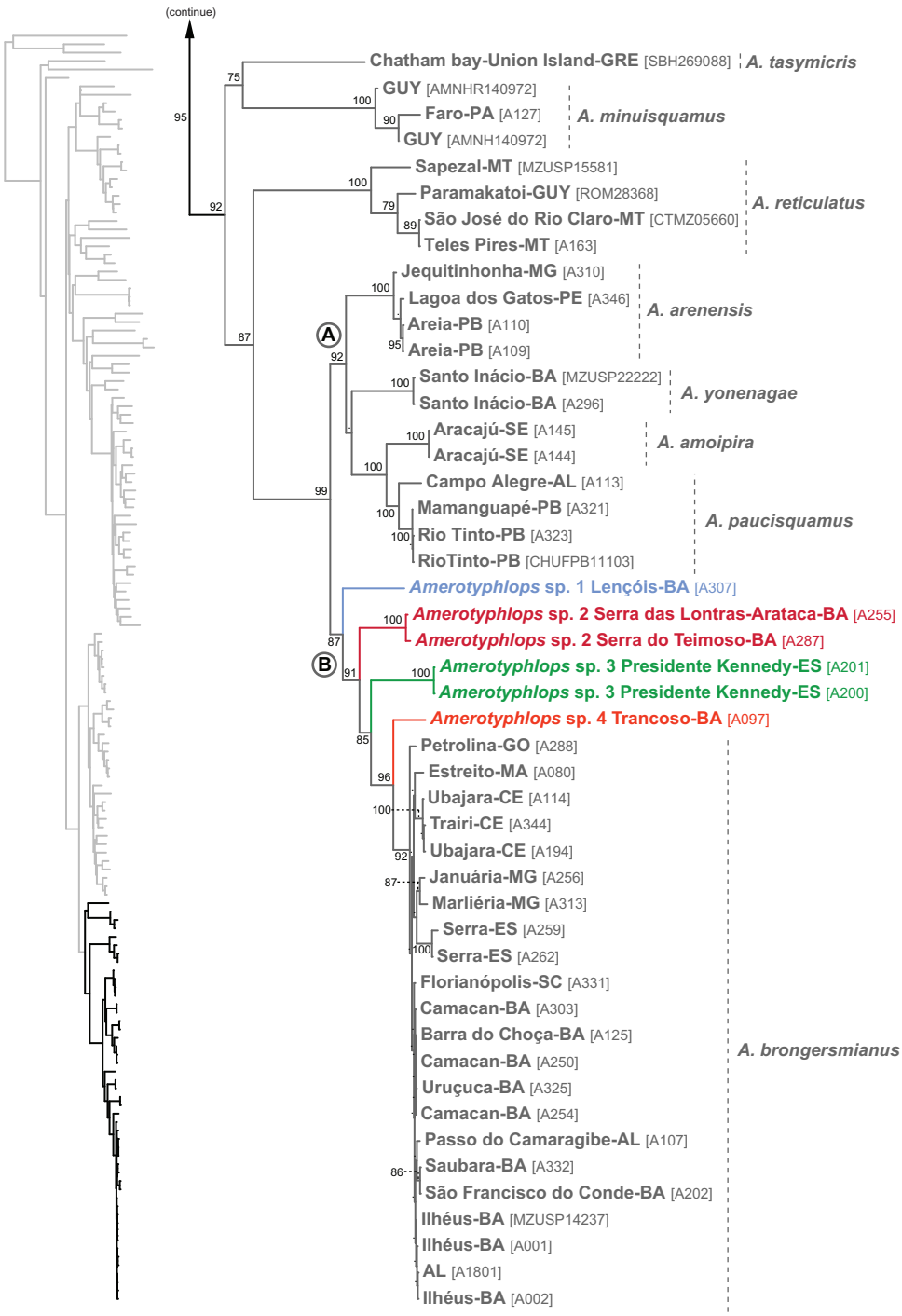

Figure 1. Maximum likelihood tree of Typhlopoidea zoomed into the South American radiation of *Amerotyphlops*. The numbers on the branch represent bootstrap values > 75%. Letter A indicates the species of northern Brazil (Clade A), and letter B indicates species of the *Amerotyphlops brongersmianus* species complex (Clade B). Colour on branch represents the cryptic species *Amerotyphlops* sp. 1 (light blue), *Amerotyphlops* sp. 2 (dark pink), *Amerotyphlops* sp. 3 (green), and *Amerotyphlops* sp. 4 (red).

datasets showed a small overlap of variables between *A. amoipira*, *A. arenenesis* and *A. paucisquamus* within the GR1 (Supporting Information, Fig. S2A), while in GR2 we observed a large overlap of variables only between *A. brongersmianus* and *A.* sp. 4 (Supporting Information, Fig. S2B).

Results obtained by PLS-DA and LDA, based on a simulated dataset, also recognize the two higher

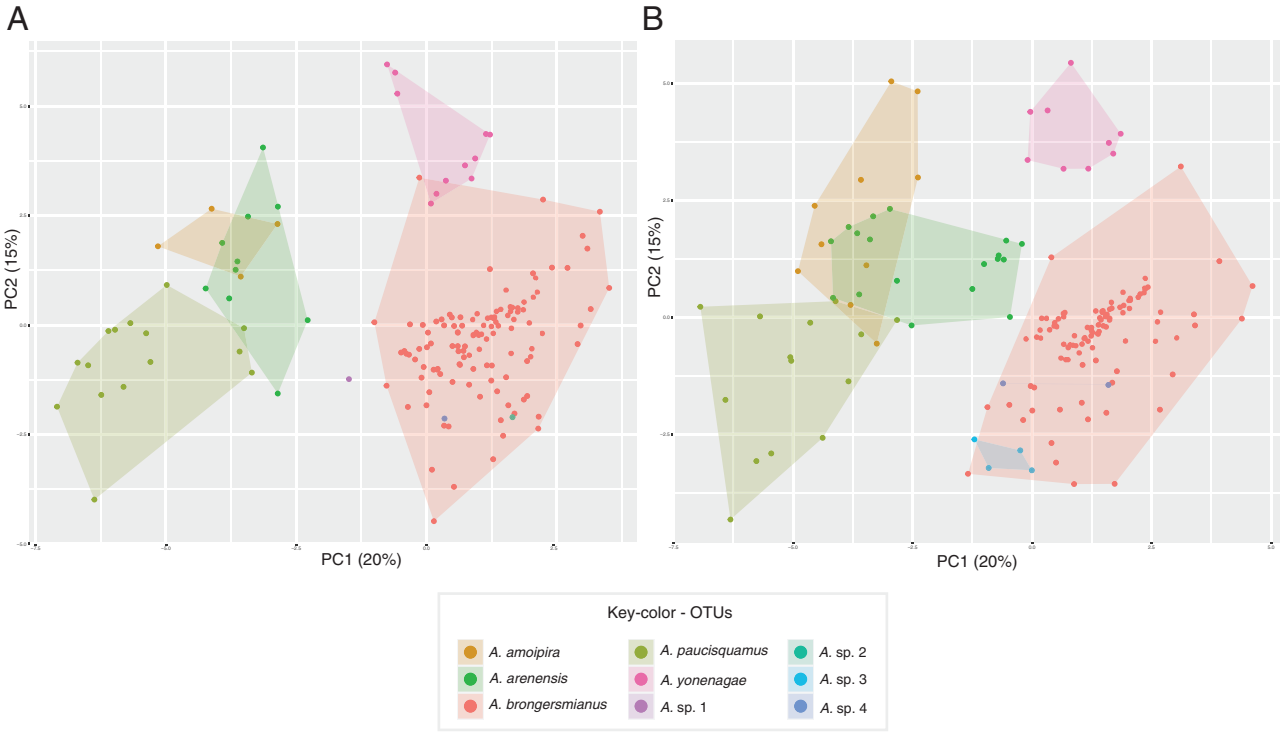

Figure 2. Results of principal component analysis (PCA) using the raw dataset based on 36 characters for nine OTUs. A, PCA of females. B, PCA of males. Species are colour-coded according to OTUs (see Key-colour OTUs, on the bottom).

groups mentioned above (GR1 and GR2), separated by the first and second components (Fig. 3A–D). In the PLS-DA using 22 variables (discrete and ratios), the first two components explained 83.3% (43.5% and 39.8%, respectively) of the total variance for GR1 (Fig. 3A), and the first two components explained 63.9% (36.6% and 27.3%, respectively) of the total variance for GR2 (Fig. 3B). In the LDA using 14 variables (continuous), based on the simulated dataset, the first two linear discriminants explained 81% (60% and 21%, respectively) of the total variance for GR 1 (Fig. 3C), and the first two linear discriminants explained 89% (61% and 28%, respectively) of the total variance for GR2 (Fig. 3D). The results obtained by PLS-DA and LDA also showed a small overlap of variables between *A. amoipira*, *A. arenensis* and *A. paucisquamus* within the GR1, while in GR2 we also observed a large overlap of variables only between *A. brongersmianus* and *A.* sp. 4 (Fig. 3A, B, D). However, the results obtained by LDA showed a large overlap of *A. arenensis* with all OTUs within GR1 (Fig. 3C).

Additionally, the results obtained in an exploratory MANOVA-NP (we used PerMANOVA as implemented in the R package *vegan*) based on the simulated dataset indicated that the morphological variation among OTUs is significantly different (see Supporting Information, Table S11). The *P*-values for the pair-wise difference among OTUs were highly significant for most comparisons ($P > 0.01$ and $P > 0.05$), except between *A. brongersmianus* and *A.* sp. 4 ($P = 0.86$; Supporting Information, Table S11).

Species accounts

Based on the results of our phylogenetic tree, in combination with estimated patristic distances and multivariate morphological analyses, we were able to recognize four new species of South American *Amerotyphlops*. We formally describe them below.

Amerotyphlops caetanoi sp. nov.

(Fig. 4; Supporting Information, Fig. S3)

Zoobank registration: LSIDurn:lsid:zoobank.org:act:BA5C7CBF-7391-4797-8CEC-DF201B294A73

Holotype: An adult female, MZUSP S-023380, (field number MTR 19921), collected by Ana C. Q. Carnaval, José C. Silva, Marco A. Sena, Mauro Teixeira Jr., Miguel T. Rodrigues, Renata C. Amaro and Renato Recoder on 15 December 2010 from Parque Nacional da Chapada Diamantina, on BR 144 Road, municipality Lençóis (12° 32′ 44.682″ S, 41° 21′ 50.364″ W; *c.* 493 m a.s.l.), state of Bahia, Brazil (Fig. 4; Supporting Information, Fig. S3).

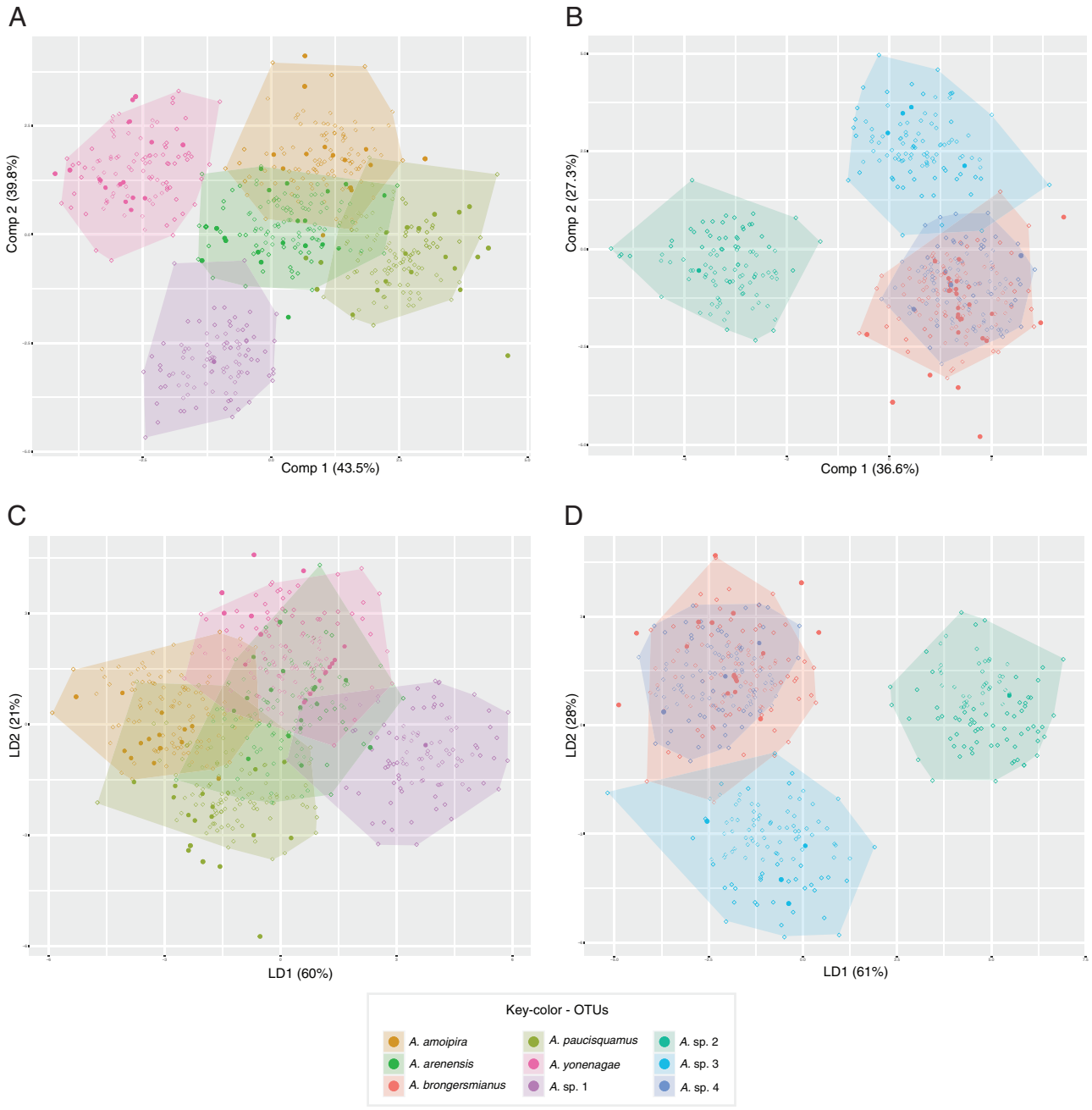

Figure 3. Results of partial least square discriminant analysis (PLS-DA) and linear discriminant analysis (LDA). A, PLS-DA of the simulated dataset based on seven discrete (pholidosis) and 14 rates characters for five OTUs (Group 1). B, PLS-DA of the simulated dataset based on seven discrete (pholidosis) and 14 rates characters for four OTUs (Group 2). C, LDA of the simulated dataset based on 15 continuous (linear morphometrics) characters for five OTUs (Group 1). D, LDA of the simulated dataset based on 15 continuous (linear morphometrics) characters for four OTUs (Group 2). Species are colour-coded according to OTUs (see Key-colour OTUs, on the bottom).

Diagnosis: This species is distinguished from all other congeneric species by the unique combination of the following of characters: (1) nasal suture incomplete; (2) rostral scale oval; (3) supralabial scales four; (4) infralabial scales three; (5) rows scales around the body 18/18/18; (6) mid-dorsal scales 212; (7) ventral scales 202; (8) rows of dorsal scales dark brown 13; (9) rows of ventral scales yellowish cream and immaculate 5; (10) caudal spine dark brown; (11) subcaudal scales 9; (12) TTL 176 mm; (13) TL 4.33 mm; (14) broad contact between the lamina of the premaxilla and the vertical laminae of the nasals, forming a continuous

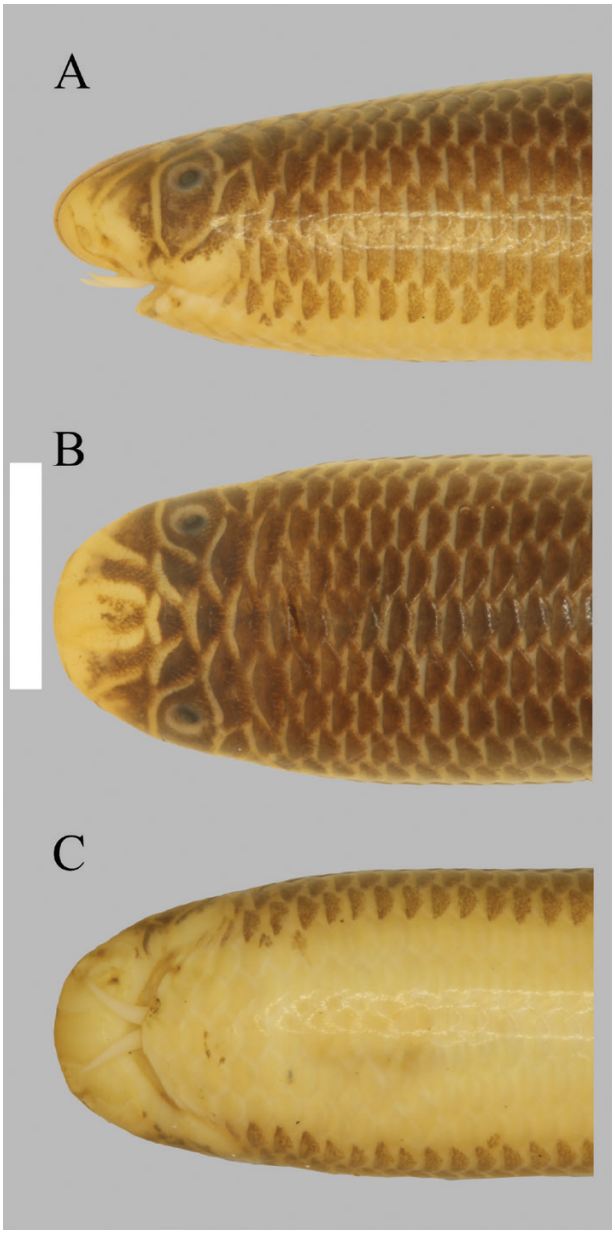

Figure 4. Holotype of *Amerotyphlops caetanoi* sp. nov. (MZUSP S-023380). Head in left lateral (A), dorsal (B) and ventral (C) views. TTL = 176 mm. Scale bar equal to 5 mm.

bony septum separating the olfactory chambers; (15) large palatine fossa on the lateral side of the maxilla; (16) maxilla with a straight medial border; (17) ventral pterygoid process of palatine straight; (18) ratio between length of ventral pterygoid process of palatine and skull length 0.25; (19) angle between mandibular condyle articulation and the retroarticular process of the compound bone close to 90°; and (20) dorsal surface of dentary bone with two evident foramina.

The new species differs from *Amerotyphlops costaricensis*, *A. lehneri*, *A. microstomus*, *A. stadelmani*, *A. tasymicris*, *A. tenuis*, *A. trinitatus* and *A. tycherus*, by having an incomplete nasal suture (vs. complete nasal suture); from *A. brongersmianus*, *A. reticulatus* and *A. minuisquamus* by having 18/18/18 rows scales around the body (vs. 18/16/14, 18/18/14, 20/18/14 or 20/18/15 in *A. minuisquamus*; 20/20/18 or 20/20/20 in *A. brongersmianus* and *A. reticulatus*); from *A. brongersmianus* by having an angle close to 90° between mandibular condyle articulation and the retroarticular process of the compound bone (vs. an angle of 135°); from *A. yonenagae* by having less than 250 mid-dorsal scales (vs. more than 250 mid-dorsal); from *A. amoipira* by having highly pigmented cephalic scales with a dark brown dorsum (vs. few pigmented cephalic scales, creamy brown dorsum with a fine darker brown paravertebral line concentrated in the anterior part of the body); from *A. paucisquamus* by having a largest number of mid-dorsal, 212 (vs. fewer number of mid-dorsal, between 162 and 209); and from *A. arenensis* by having a smaller rostral width (RW1) at dorsal portion, 1.29 mm (vs. larger rostral width at dorsal portion (RW1), between 1.44 and 2.13 mm). Table 1 shows additional morphometric characters and scale patterns found in *A. caetanoi* and morphologically similar species distributed in southern and north-eastern Brazil.

Description of the holotype: Adult female, TTL 176 mm, TL 4.33 mm, MBD/(SVL-HR) 0.036 mm, and TL/SVL 39.72 mm. Head slightly depressed dorsoventrally, not wider than 'neck'. Snout round in dorsal and ventral views. Rostral oval, longer than wide, narrow at anteroposterior region and wider at medial region; visible in dorsal view, extending ventrodorsally without reaching the imaginary transverse line between anterior borders of eyes. Rostral contacting nasal (anterior and posterior) dorsolaterally, and first supralabial and anterior nasal scales ventrally. Nasal suture incomplete, only partially dividing the anterior and posterior portions of nasal scale. Suture begins in the upper edge of second supralabial, passes through nostril, but fails to reach rostral. Anterior nasal in contact with first infralabial and upper edge of second infralabial. Posterior nasal longer than wide, contacting upper margin of second supralabial and preocular. Supralabials four, fourth twice longer than third. Infralabials three, third largest. Eye diameter 0.56 mm; eyes not visible in ventral view, located dorsolaterally, close to suture between preocular and ocular scales, completely covered by ocular scale. Ocular scales contacting frontal. Body cylindrical and robust. Midbody diameter 6.21 mm. Dorsal and ventral scales cycloid, wider than long, highly imbricated and arranged in diagonal series; scale rows around the body 18/18/18. Mid-dorsal scales 212. Ventral scales 202. Cloacal plate rounded, bordered anteriorly by four

Table 1. Variation for selected characters of morphologically similar species of *Amerotyphlops* from Brazil. Values displayed in the table represent (in this sequence) range (mm), mean, standard deviations and available sample size.

Character	Sex	*A. arenensis*	*A. brongersmianus*	*A. martis*	*A. montanum*	*A. caetanoi*	*A. illusorium*
ED	♂	0.9 ± 0.13 (0.61–1.05) 12	0.99 ± 0.27 (0.40–1.69) 39	0.76 ± 0.21 (0.63–1.16) 4	1.03 ± na (1.02) 1	-	0.72 ± 0.01 (0.71–0.72) 2
	♀	0.94 ± 0.14 (0.78–1.21) 9	1.03 ± 0.26 (0.61–1.72) 63	-	-	0.56 ± na (0.56) 1	0.77 ± na (0.77) 1
HR	♂	2.98 ± 0.13 (2.73–3.13) 12	3.56 ± 0.55 (2.77–4.78) 39	2.30 ± 0.17 (2.61–3.05) 4	3.88 ± na (3.88) 1	-	3.03 ± 0.57 (2.63–3.43) 2
	♀	3.24 ± 0.18 (2.97–3.50) 9	3.80 ± 0.56 (2.87–5.39) 63	-	-	2.86 ± na (2.86) 1	3.78 ± na (3.78) 1
HWE	♂	5.04 ± 0.41 (4.37–5.54) 12	5.75 ± 0.99 (4.10–8.17) 39	3.24 ± 0.12 (3.84–4.10) 4	6.64 ± na (6.64) 1	-	4.66 ± 0.65 (4.20–5.12) 2
	♀	5.52 ± 0.43 (4.80–6.06) 9	6.12 ± 1.02 (4.45–8.62) 63	-	-	4.44 ± na (4.44) 1	5.75 ± na (5.75) 1
IN	♂	2.41 ± 0.19 (2.08–2.65) 12	2.77 ± 0.45 (1.84–3.59) 39	1.68 ± 0.13 (1.89–2.22) 4	2.63 ± na (2.63) 1	-	2.32 ± 0.18 (2.19–2.45) 2
	♀	2.63 ± 0.22 (2.35–3.00) 9	2.92 ± 0.45 (2.16–4.14) 63	-	-	2.16 ± na (2.16) 1	2.82 ± na (2.82) 1
INORB	♂	3.25 ± 0.17 (2.87–3.45) 12	3.55 ± 0.6 (2.73–4.97) 39	2.08 ± 0.17 (2.31–2.68) 4	4.09 ± na (4.09) 1	-	3.00 ± 0.57 (2.60–3.40) 2
	♀	3.45 ± 0.25 (3.00–3.83) 9	3.68 ± 0.57 (2.72–5.11) 63	-	-	2.90 ± na (2.90) 1	3.90 ± na (3.9) 1
RL	♂	2.76 ± 0.23 (2.26–3.09) 12	3.22 ± 0.54 (2.27–4.37) 39	1.95 ± 0.19 (2.23–2.66) 4	3.15 ± na (3.15) 1	-	2.61 ± 0.25 (2.44–2.79) 2
	♀	3.11 ± 0.26 (2.71–3.54) 9	3.37 ± 0.53 (2.47–4.80) 63	-	-	2.51 ± na (2.51) 1	3.12 ± na (3.12) 1
RW1	♂	1.63 ± 0.09 (1.44–1.77) 12	1.76 ± 0.27 (1.27–2.37) 39	1.12 ± 0.09 (1.23–1.44) 4	1.88 ± na (1.88) 1	-	1.33 ± 0.16 (1.22–1.44) 2
	♀	1.77 ± 0.18 (1.56–2.13) 9	1.89 ± 0.30 (1.34–1.2.70) 63	-	-	1.29 ± na (1.29) 1	1.54 ± na (1.54) 1
MBD	♂	6.82 ± 1.11 (4.81–7.86) 12	8.14 ± 1.99 (5.03–14.47) 39	3.83 ± 0.44 (4.09–5.13) 4	7.12 ± na (7.12) 1	-	5.01 ± 0.14 (4.92–5.11) 2
	♀	8.03 ± 1.03 (5.93–8.98) 9	8.87 ± 2.15 (5.82–14.76) 63	-	-	6.21 ± na (6.21) 1	8.29 ± na (8.29) 1
INORB/HWE	♂	0.65 ± 0.03 (0.61–0.71) 12	0.62 ± 0.04 (0.55–0.71) 39	0.51 ± 0.02 (0.60–0.66) 4	0.72 ± na (0.72) 1	-	0.64 ± 0.03 (0.62–0.66) 2
	♀	0.62 ± 0.02 (0.58–0.66) 9	0.60 ± 0.04 (0.53–0.69) 63	-	-	0.66 ± na (0.66) 1	0.68 ± na (0.68) 1
NE/HWE	♂	0.41 ± 0.02 (0.38–0.44) 12	0.38 ± 0.02 (0.35–0.41) 39	0.33 ± 0.04 (0.36–0.46) 4	0.49 ± na (0.49) 1	-	0.39 ± 0.01 (0.39–0.40) 2
	♀	0.41 ± 0.02 (0.39–0.44) 9	0.39 ± 0.03 (0.33–0.47) 63	-	-	0.39 ± na (0.39) 1	0.42 ± na (0.42) 1

Abbreviations: ED, eye diameter; HR, head radius; HWE, head width; IN, internasal distance; INORB, interorbital distance; RL, rostral length; RW1, rostral width; MBD, midbody diameter.

rows of scales and posteriorly by five rows of scales. Subcaudal scales nine, excluding the terminal spine. Terminal spine large, stout base and dark brown.

*Skull osteology (*N = 1*; MZUSP S-023380):* The length of the skull is 6.15 mm, the width is 2.92 mm. The snout region has a globular enlarged-shape and highly consolidated. The snout articulates with the braincase by the nasal and prefrontal sutures and with the frontal bone. The anteroventral region of the premaxilla has a short backward process. The midsagittal lamina separates both sides of the premaxilla (Fig. 5). The lamina of the premaxilla is confluent with the mid-dorsal laminae of the nasals and with the mid-dorsal ridges of the vomeronasal cupola of the septomaxillae (Fig. 5). The lamina of the premaxilla and the nasal laminae are in contact, forming a continuous bony septum separating the olfactory chambers (Fig. 5B). The medial side of the maxilla has a shallow depression (or fossa), where lodges the maxillary process of the palatine. The palatine fossa is on the lateral side of the maxilla, in the region of the articular fossa. The palatine fossa is large with a diameter of 0.25 mm long (Fig. 6A). The medial border of the maxilla is straight (Fig. 6A). The ventral pterygoid process of the palatine is straight and ventrally directed (Fig. 7A). The retroarticular process projects in parallel to the horizontal plane of the articular. The angle between mandibular condyle articulation and the retroarticular process of the compound bone is close to 90° (Fig. 8A). The edentulous dentary is restricted to the distal end of the mandible, articulating mainly with the splenial. The dorsal side of the dentary is flat and pierced by two foramina (Fig. 9A).

Coloration of the holotype in preservative: Dorsum (13/13/13 row scales) dark brown (Supporting Information, Fig. S3A), venter (5/5/5 rows scales) yellowish cream (Supporting Information, Fig. S3B). Dorsal portions of snout yellowish cream, with a dark brown spot, covering both rostral and nasal scales (two-thirds of snout) (Fig. 4A, B). Ventral portions of snout yellowish cream and few pigmented (Fig. 4C). Symphysial region yellowish cream and immaculate (Fig. 4C). Dorsal head scales (supraoculars, frontal, postfrontal, parietals and occipitals) dark brown. Dorsal portions of lateral head scales (ocular, nasal and lower nasal) and ventral portions yellowish cream with dark brown spots. Cloacal plate pale yellowish cream and terminal spine dark brown (Fig. 4A–C).

Etymology: The name is a homage to Brazilian composer, singer and political activist Caetano Emanuel Viana Telles Veloso, better known as Caetano Veloso. Caetano is one of the most famous Brazilians born in the state of Bahia (in 1942), the same state in which the new species occurs. He became known for his participation in the Brazilian musical movement '*Tropicalismo*' that encompassed theatre, poetry and music in the 1960s, at the beginning of the Brazilian military dictatorship. Veloso is also a well-known conservationist, acting to give voice to the preservation of the Brazilian natural environments and to indigenous resilience.

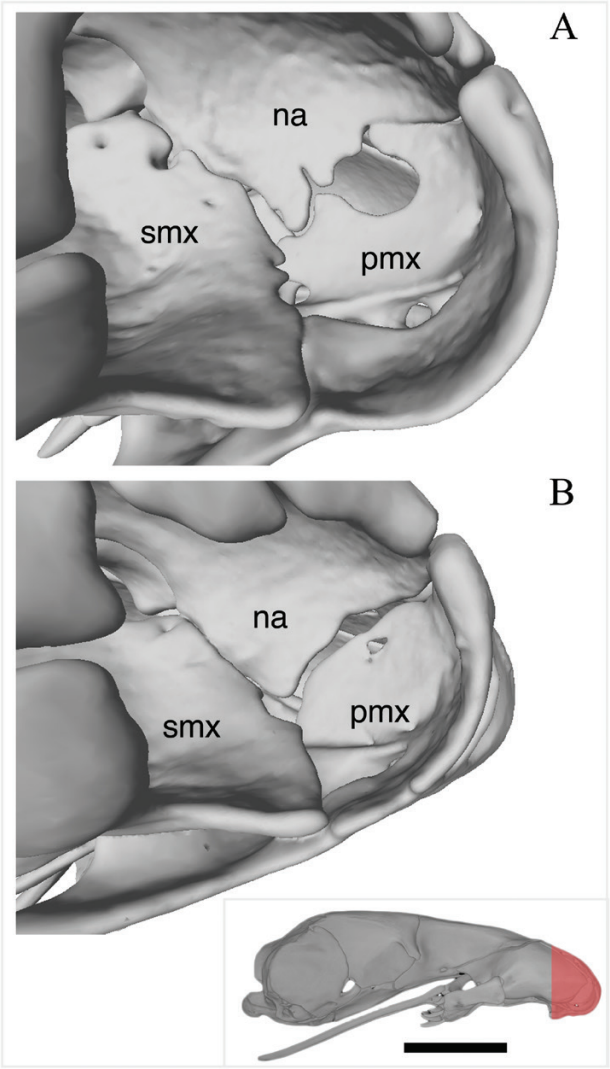

Figure 5. Three-dimensional cutaway views along the sagittal axis of the nasal cavity in *Amerotyphlops* species based on HRXCT data. A, *Amerotyphlops brongersmianus* (MZUSP 14689); B, *Amerotyphlops caetanoi* sp. nov. (MZUSP S-023380). Insert show a lateral profile of the skull of *A. brongersmianus* presenting in red the position of the detailed region. Scales bars equal to 5 mm. Abbreviations: pmx, premaxilla; smx, septomaxilla; vm, vomer; na, nasal.

Distribution and habitat: Amerotyphlops caetanoi is known only from Parque Nacional da Chapada

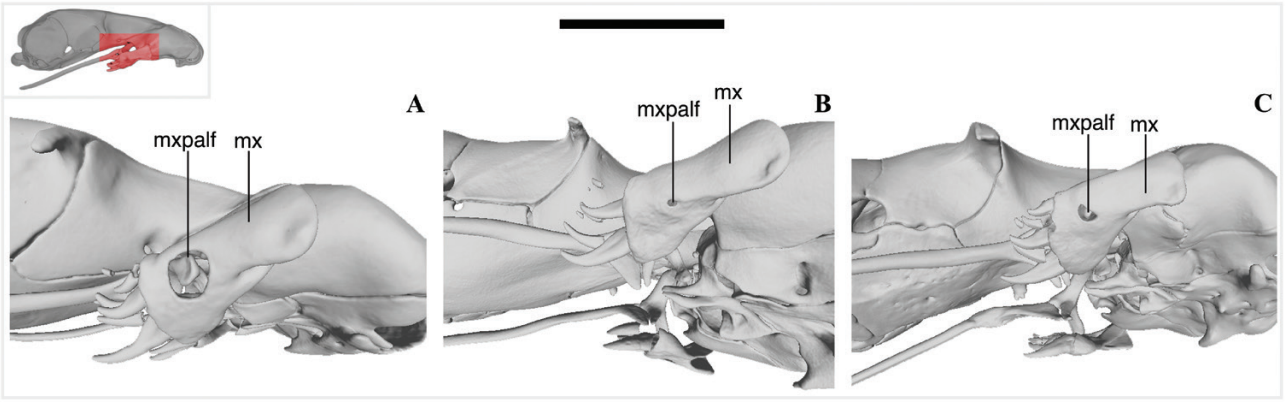

Figure 6. Three-dimensional reconstruction of the lateral region of the skull in *Amerotyphlops* species based on HRXCT data. A, *Amerotyphlops caetanoi* sp. nov. (MZUSP S-023380); B, *Amerotyphlops montanum* sp. nov. (MZUSP 20065); C, *Amerotyphlops brongersmianus* (MZUSP 14674). Insert shows a lateral profile of the skull of *A. brongersmianus* presenting in red the position of the detailed region. Scales bars equal to 5 mm. Abbreviations: mx, maxilla; mxpalf, palatine articulation fossa of the maxilla.

Diamantina, in the BR 144 Road, situated at 2 km from the municipality of Lençóis, state of Bahia, Brazil (Fig. 10B). This region is one of the largest upland Atlantic dry forest enclaves of the east-central Bahia state (Veloso *et al.*, 1991). The phytophysiognomy corresponds to a submontane seasonal semi-deciduous forest (Couto *et al.*, 2011; Braz *et al.*, 2013), ranging from 400 to 600 m a.s.l., with an annual average of temperature and rainfall of 20 °C and 100 mm, respectively (Funch *et al.*, 2009). This area presents a non-continuous canopy, consisting of tall trees (approximately 10–16 m), and a subcanopy, consisting of medium-height trees (approximately 6–9 m), with a well-established and preserved understory (Couto *et al.*, 2011).

AMEROTYPHLOPS MONTANUM SP. NOV.

(FIG. 11; SUPPORTING INFORMATION, FIG. S4)

Zoobank registration: urn:lsid:zoobank.org:act:BDB85DE5-C88C-4894-9197-60C3200FEC73

Holotype: An adult female, MZUSP 20065, (field number MTR 16379), collected by Augustín Camacho, José Cassimiro, Mauro Teixeira Jr., Miguel T. Rodrigues, Renata C. Amaro and Renato Recoder 6 March 2009 from Parque Nacional Serra das Lontras (15° 11′ 46.32″ S, 39° 20′ 54.24″ W; *c.* 234 m a.s.l.), municipality of Arataca, state of Bahia, Brazil (Fig. 11; Supporting Information, Fig. S4).

Diagnosis: This species is distinguished from all other South American congeneric species by a unique combination of the following of characters: (1) nasal suture incomplete; (2) rostral scale oval; (3) supralabial scales four; (4) infralabial scales three; (5) rows scales around the body 20/20/18; (6) mid-dorsal scales 220; (7) ventral scales 217; (8) rows of dorsal scales dark brown 11; (9) rows of ventral scales yellowish cream and immaculate 7–9; (10) caudal spine dark brown; (11) subcaudal scales 11; (12) TTL 216 mm; (13) TL 5.32 mm; (14) contact between the nasal process of premaxilla and vertical laminae of the nasals restricted to the anterodorsal portion, with the central and posteroventral portions not in contact, leaving a large canal between the olfactory chambers; (15) small-sized palatine fossa on the lateral side of the maxilla; (16) maxilla with a straight medial border; (17) ventral pterygoid process of palatine straight; (18) ratio between length of ventral pterygoid process of palatine and skull length 0.06; (19) angle between mandibular condyle articulation and the retroarticular process of the compound bone close to 90°; and (20) dorsal surface of dentary bone without evident foramina.

Amerotyphlops montanum differs from *A. costaricensis*, *A. lehneri*, *A. microstomus*, *A. stadelmani*, *A. tasymicris*, *A. tenuis*, *A. trinitatus* and *A. tycherus* by having an incomplete nasal suture (vs. complete nasal suture); from *A. arenensis, A. caetanoi*, *A. amoipira*, *A. minuisquamus*, *A. paucisquamus* and *A. yonenagae* by having 20/20/18 rows scales around the body (vs. 18/16/14, 18/18/14, 20/18/14 or 20/18/15 in *A. minuisquamus* and 18/18/18 in *A. arenensis, A. caetanoi*, *A. amoipira*, *A. paucisquamus* and *A. yonenagae*); from *A. reticulatus* by having highly pigmented cephalic scales with a dark brown dorsum and dorsum tail brown (vs. yellow and few pigmented cephalic scales, dorsum brown or black and dorsum tail black with cream or yellow spot); and

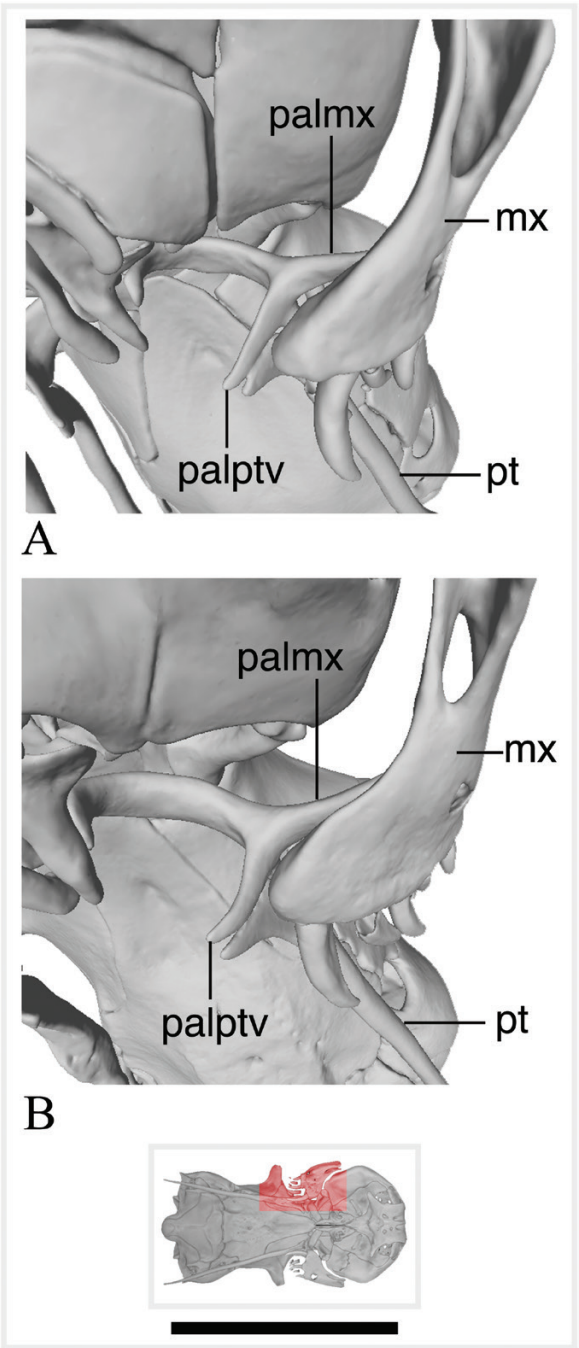

Figure 7. Three-dimensional reconstruction of the latero-ventral region of the skull in *Amerotyphlops* species based on HRXCT data. A, *Amerotyphlops caetanoi* sp. nov. (MZUSP S-023380); B, *Amerotyphlops brongersmianus* (MZUSP 14674). Insert shows a lateral profile of the skull of *A. brongersmianus* presenting in red the position of the detailed region. Scales bars equal to 5 mm. Abbreviations: mx, maxilla; palmx, palatine maxillary process; palptv, palatine pterygoid ventral process; pt, pterygoid.

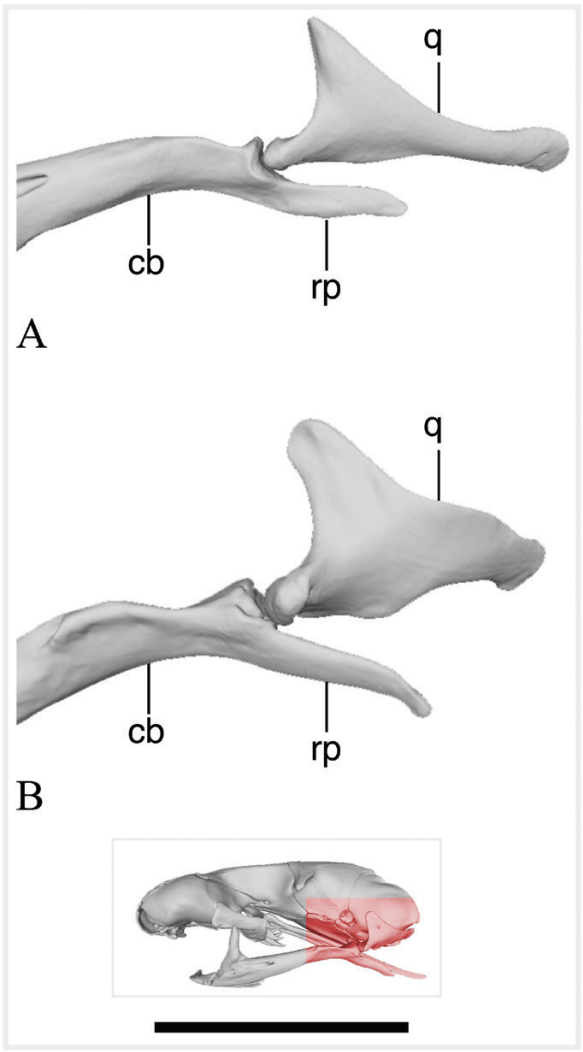

Figure 8. Three-dimensional reconstruction of the posterior region of the left mandible in *Amerotyphlops* species based on HRXCT data. A, *Amerotyphlops caetanoi* sp. nov. (MZUSP S-023380); B, *Amerotyphlops brongersmianus* (MZUSP 14674). Insert shows a lateral profile of the skull of *A. brongersmianus* presenting in red the position of the detailed region. Scales bars equal to 5 mm. Abbreviations: cb, compound bone; q, quadrate; rp, retroarticular process.

from *A. brongermianus* by having a larger interorbital relative width (INORB/HWE) 0.725 mm (vs. smaller interorbital relative width, between 0.526–0.705 mm). Table 1 shows additional morphometric characters and scale patterns found in *A. montanum* and in a morphologically similar species distributed in south-eastern Brazil (*A. brongermianus*).

Description of the holotype: Adult female, TTL 216 mm, TL 5.32 mm, MBD/(SVL-HR) 0.034 mm and TL/SVL

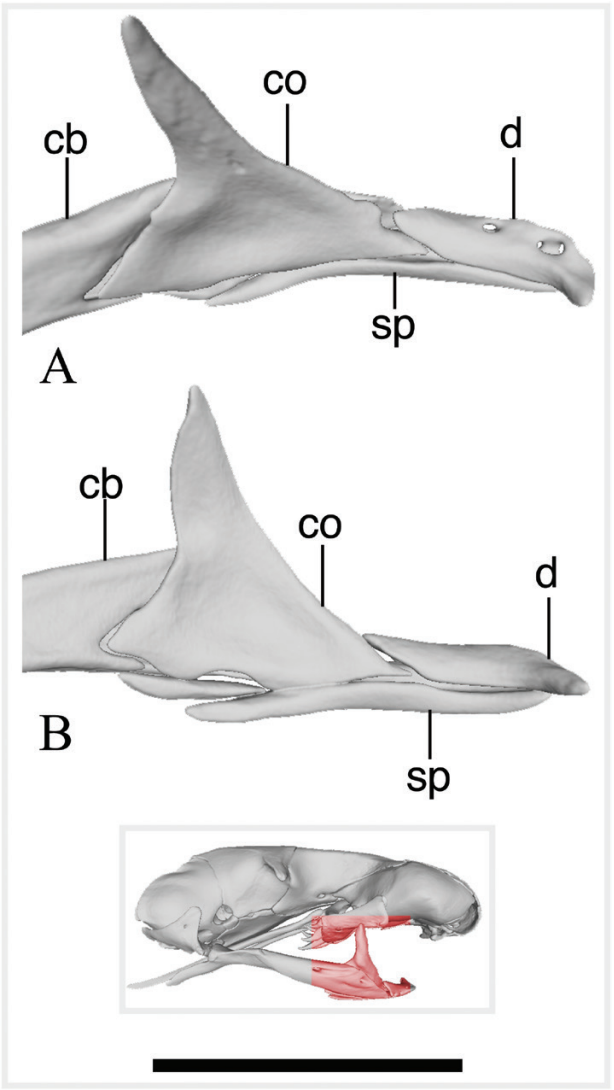

Figure 9. Three-dimensional reconstruction of the anterior region of the left mandible in *Amerotyphlops* species based on HRXCT data. A, *Amerotyphlops caetanoi* sp. nov. (MZUSP S-023380); B, *Amerotyphlops montanum* sp. nov. (MZUSP 20065). Insert shows a lateral profile of the skull of *A. brongersmianus* presenting in red the position of the detailed region. Scales bars equal to 5 mm. Abbreviations: cb, compound bone; co, coronoid; d, dentary; sp, splenial.

39.60 mm. Head slightly depressed dorsoventrally, not wider than 'neck'. Snout round in dorsal and ventral views. Rostral oval, longer than wide, narrow at anteroposterior region and wider at medial region; visible in dorsal view, extending ventrodorsally without reaching the imaginary transverse line between anterior borders of eyes. Rostral contacting nasal (anterior and posterior) dorsolaterally, and first supralabial and anterior nasal scales ventrally. Nasal suture incomplete, only partially dividing the anterior and posterior portions of nasal scale. Suture begins in the upper edge of second supralabial, passes through nostril, but fails to reach rostral. Anterior nasal in contact with first infralabial and upper edge of second infralabial. Posterior nasal longer than wide, contacting upper margin of second supralabial and preocular. Supralabials four, fourth twice longer than third. Infralabials three, third largest. Eye diameter 1.03 mm; eyes not visible in ventral view, located dorsolaterally, close to suture between preocular and ocular scales, completely covered by ocular scale. Ocular scales contacting frontal. Body cylindrical and robust. Midbody diameter 7.12 mm. Dorsal and ventral scales cycloid, wider than long, highly imbricated and arranged in diagonal series; scale rows around the body 20/20/18. Mid-dorsal scales 220. Ventral scales 217. Cloacal plate rounded, bordered anteriorly by four rows of scales and posteriorly by five rows of scales. Subcaudal scales 11, excluding the terminal spine. Terminal spine large, stout base and dark brown.

*Skull osteology (*N = 1*; MZUSP 20065):* The length of the skull is 8.08 mm and the width is 4.14 mm. The snout region has a globular enlarged-shape and highly consolidated. The snout articulates with the braincase by the nasal and prefrontal sutures and with the frontal bone. The anteroventral region of the premaxilla has a short backward process. The midsagittal lamina separates both sides of the premaxilla (Fig. 5). The lamina of the premaxilla is confluent with the mid-dorsal laminae of the nasals and with the mid-dorsal ridges of the vomeronasal cupola of the septomaxillae (Fig. 5). The lamina of the premaxilla and the nasal laminae are restricted to the anterodorsal portion, with the central and posteroventral portions not in contact, leaving a large canal between the olfactory chambers (Fig. 5A). The medial side of the maxilla has a shallow depression (or fossa), where lodges the maxillary process of the palatine. The palatine fossa is on the lateral side of the maxilla, in the region of the articular fossa. The palatine fossa is small, with a diameter of 0.17 mm long (Fig. 5B). The medial border of the maxilla is straight (Fig. 6B). The ventral pterygoid process of the palatine is straight-shaped and ventrally directed (Fig. 7A). The retroarticular process projects in parallel to the horizontal plane of the articular. The angle between mandibular condyle articulation and the retroarticular process of the compound bone is close to 90° (Fig. 8A). The edentulous dentary is restricted to the distal end of the mandible, articulating mainly with the splenial. The dorsal side of the dentary is flat and without evident foramina (Fig. 9B).

Coloration of the holotype in preservative: Dorsum (11/11/11 rows scales) dark brown, venter (9/9/7 rows scales) yellowish cream (Supporting Information, Fig. S4A, B). Dorsal portions of snout yellowish cream,

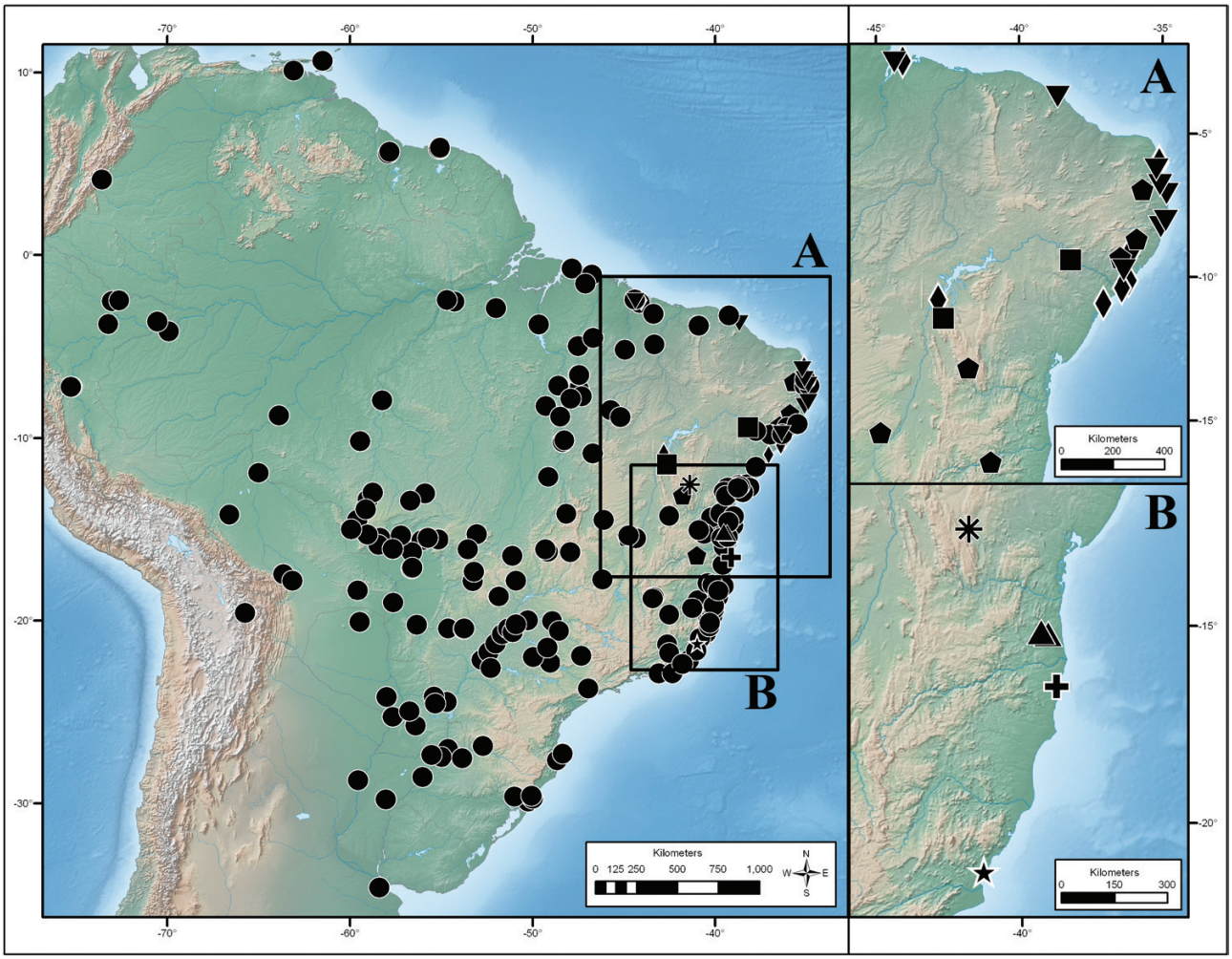

Figure 10. Geographical distribution of nine species belonging to the genus *Amerotyphlops* from South America. A, zoomed map of species distributed in the north-eastern Brazil; B, zoomed map of four new species described in this work. Symbols: *A. arenensis* (black pentagons); *A. amoipira* (black diamonds); *A. brongersmianus* (black circles); *A. yonenagae* (black squares); *A. pauciquamus* (black inverted triangles); *A. martis* sp. nov. (black star); *A. montanum* sp. nov. (black triangles); *A. illusorium* sp. nov. (black cross); *Amerotyphlops caetanoi* sp. nov. (black asterisk).

with a dark brown spot, covering totally both rostral and nasal scales (Fig. 11A, B). Ventral portion of snout yellowish cream and few pigmented (Fig. 11C). Symphysial region yellowish cream and immaculate (Fig. 11C). Dorsal head scales (supraoculars, frontal, postfrontal, parietals and occipitals) and dorsal portions of lateral head scales (ocular, nasal and lower nasal) predominantly dark brown (Fig. 11A, B). Ventral portion of head scales (nasal and lower nasal) yellowish cream (Fig. 11A, C). Cloacal plate pale yellowish cream and terminal spine dark brown (Supporting Information, Fig. S4B).

Etymology: The specific epithet is derived from the neutral form of Latin adjective '*montanus*'. It is a reference to the type locality, a high elevational forest, located on the slopes of a hill summit in the Brazilian state of Bahia.

Distribution and habitat: Amerotyphlops montanum is known from the Parque Nacional Serra das Lontras, situated at 10 km from the municipality of Arataca, in state of Bahia, Brazil, and from Reserva Particular do Patrimônio Natural Serra do Teimoso, situated at 5 km from the municipality of Jussari, in state of Bahia, Brazil (Fig. 10B).

These regions are known as part of the Serra das Lontras montane complex (Nacif *et al.*, 2009), belonging to the Atlantic Forest morphoclimatic domain, in the Bahia Coastal forest ecoregion (Olson *et al.*, 2001). The prevalent phytophysiognomy correspond to ombrophilous dense and semi-deciduous forests (Veloso *et al.*, 1991; Amorim &

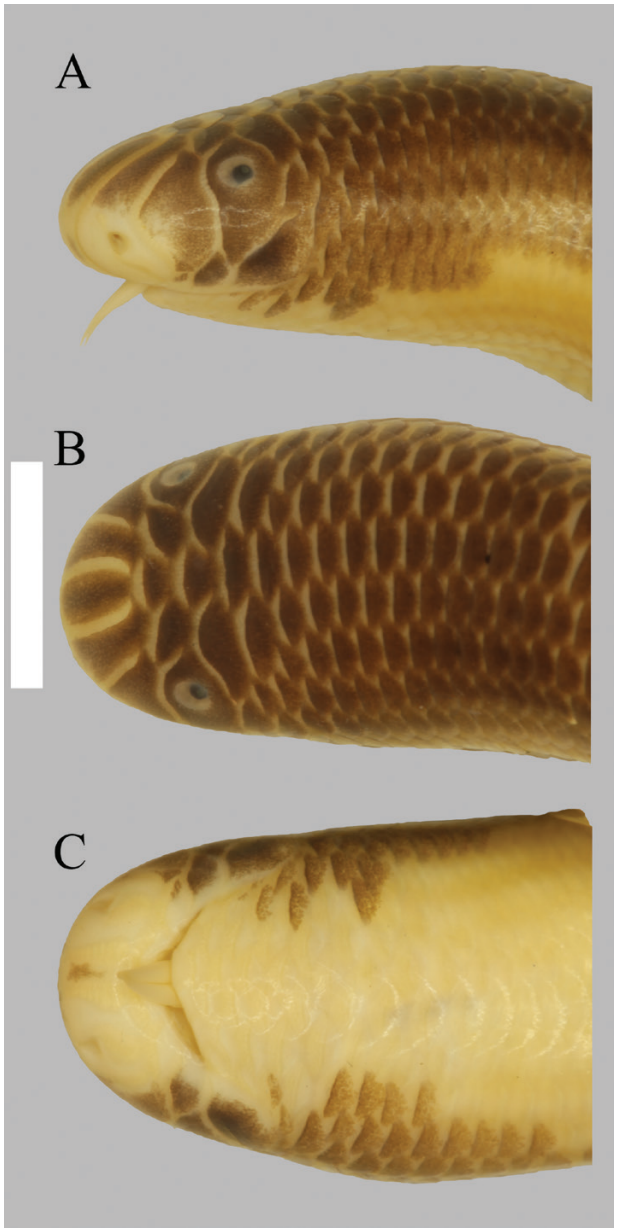

Figure 11. Holotype of *Amerotyphlops montanum* sp. nov. (MZUSP 20065). Head in left lateral (A), dorsal (B) and ventral (C) views. TTL = 216 mm. Scale bar equal to 5 mm.

Matos, 2009; Reis & Fontoura, 2009), with an elevational gradient ranging from sea level to more than 1000 m a.s.l., with an annual average of temperature between 23.3 and 23.6 °C and rainfall between 1300 and 1600 mm (Silveira *et al.*, 2005; Amorim & Matos, 2009; Nacif *et al.*, 2009; Reis & Fontoura, 2009). These areas have different levels of successional forests according to elevational gradients. Areas between 400 and 800 m, presenting a high and dense forest, with large height trees (taller than 30 m), a well-defined canopy structure, with abundant epiphytes, with a well-established and preserved understory. The forest changes dramatically above 800 m, presenting stunted trees (10–15 m tall), covered with small bromeliads, heavy bryophyte and lichen growth (Veloso *et al.*, 1991; Amorim & Matos, 2009; Reis & Fontoura, 2009). Additional data on the habitat of Serra das Lontras and Serra do Teimoso are, respectively, in Recoder *et al.* (2010) and Rodrigues *et al.* (2002).

Remarks: In our phylogenetic analysis we included a sample from a specimen from the Reserva Particular do Patrimônio Natural Serra do Teimoso, from the municipality of Jussari, in the state of Bahia, Brazil. Unfortunately, we did not have access to review this specimen, but we have recognized its molecular relationships with *A. montanum*. The tissue sample is currently stored in the genetic resource collection of Instituto de Biociências da Universidade de São Paulo University (see Supporting Information, Table S2).

AMEROTYPHLOPS MARTIS SP. NOV.

(FIG. 12; SUPPORTING INFORMATION, FIGS S5, S6)

Zoobank registration: urn:lsid:zoobank.org:act:0FDB6570-F072-4B5E-BE52-0BF93785AC88

Holotype: An adult male, MNRJ 18744, collected by Ana C. C. Lourenço and Délio Baêta between 2 and 8 September 2009 from Praia das Neves (21° 16′ 45.59″ S, 40° 57′ 47.86″ W), municipality of Presidente Kennedy, state of Espírito Santo, Brazil (Fig. 12; Supporting Information, Fig. S5).

Paratypes: Three male specimens, MNRJ 18743, MNRJ 18745 and MNRJ 18747, collected in the same locality of the holotype by Ana C. C. Lourenço and Délio Baêta between 2 and 8 September 2009 (Supporting Information, Fig. S6A–F).

Diagnosis: This species is distinguished from all other South American congeneric species by the unique combination of the following of characters: (1) nasal suture incomplete; (2) rostral scale oval; (3) supralabial scales four; (4) infralabial scales three; (5) rows scales around the body 20/20/18–20; (6) mid-dorsal scales 208–217; (7) ventral scales 195–211; (8) rows of dorsal scales pale brown 12–13; (9) rows of ventral scales yellowish cream and immaculate four to five; (10) caudal spine pale brown; (11) subcaudal scales ten to 12; (12) maximum TTL 170 mm; (13) maximum TL 6.13 mm; (14) nasal process of premaxilla contacting the vertical laminae of the nasals in the anterodorsal and posteroventral portions, with the central portion not in contact, leaving a large round canal between the olfactory chambers; (15) large palatine fossa on the lateral side of the maxilla; (16) maxilla with

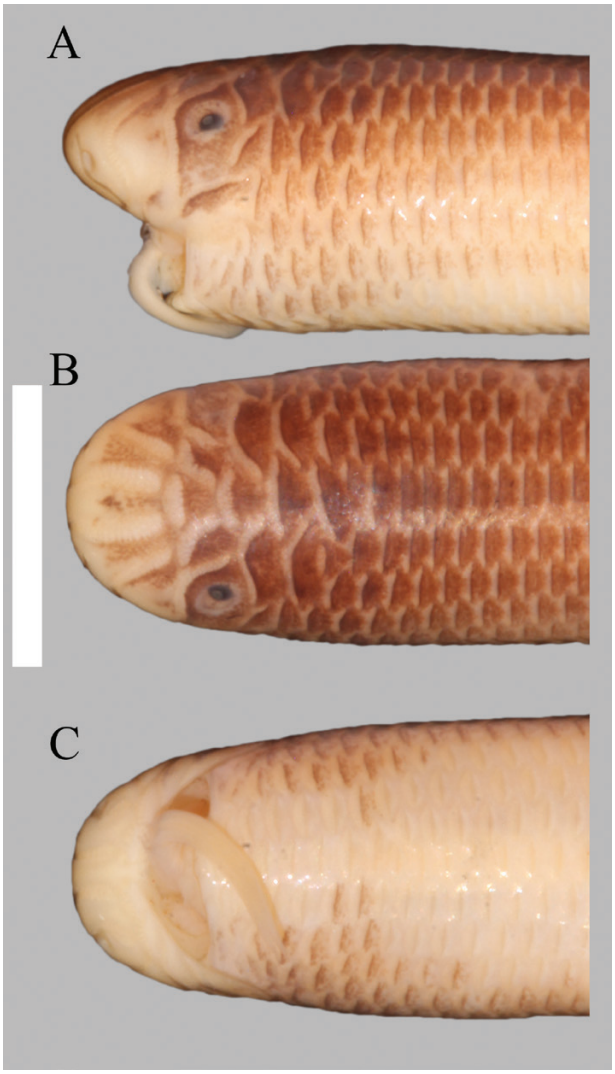

Figure 12. Holotype of *Amerotyphlops martis* sp. nov. (MNRJ 18744). Head in left lateral (A), dorsal (B) and ventral (C) views. TTL = 157 mm. Scale bar equal to 5 mm.

a concave medial border; (17) ventral pterygoid process of palatine straight; (18) ratio between length of ventral pterygoid process of palatine and skull length 0.06; (19) angle between mandibular condyle articulation and the retroarticular process of the compound bone close to 90°; (20) Dorsal surface of dentary bone with two evident foramina; and (21) hemipenis single, with an additional structure in the apical cup, with a tissue projection in the form of a curved papilla.

Amerotyphlops martis differs from *A. costaricensis*, *A. lehneri*, *A. microstomus*, *A. stadelmani*, *A. tasymicris*, *A. tenuis*, *A. trinitatus* and *A. tycherus* by having an incomplete nasal suture (vs. complete nasal suture); from *A. arenensis*, *A. caetanoi*, *A. amoipira*, *A. minuisquamus*, *A. paucisquamus* and *A. yonenagae* by having 20/20/18 or 20/20/20 rows scales around the body (vs. 18/16/14, 18/18/14, 20/18/14 or 20/18/15 in *A. minuisquamus* and 18/18/18 in *A. arenensis*, *A. caetanoi*, *A. amoipira*, *A. paucisquamus* and *A. yonenagae*); from *A. reticulatus* by having pigmented cephalic scales with a pale brown dorsum and tail (vs. a yellowish and few pigmented cephalic scales, dorsum brown or black and dorsum tail black with cream or yellow spot); from *A. montanus* by having a smaller total length (TTL), between 130 and 170 mm (vs. larger total length 216 mm); and from *A. brongermianus* by having a small midbody diameter (MBD), between 4.090 and 5.133 mm and a single hemipenis with an additional structure in the apical cup, a large papillae projected laterally from the tip that extends horizontally over the proximal portion of the apical cup (vs. robust midbody diameter, between 5.03 and 14.76 mm and a single hemipenis with an unornamented apical cup). Table 1 shows additional morphometric characters and scale patterns found in *A. martis* and morphologically similar species distributed in southern and north-eastern Brazil.

Description of the holotype: Adult male, TTL 157 mm, TL 6.13 mm, MBD/(SVL-HR) 0.032 mm and TL/SVL 24.61 mm. Head slightly depressed dorsoventrally, not wider than 'neck'. Snout round in dorsal and ventral views. Rostral oval, longer than wide, narrow at anteroposterior region and wider at medial region; visible in dorsal view, extending ventrodorsally without reaching the imaginary transverse line between anterior borders of eyes. Rostral contacting nasal (anterior and posterior) dorsolaterally and first supralabial and anterior nasal scales ventrally. Nasal suture incomplete, only partially dividing the anterior and posterior portions of nasal scale. Suture begins in the upper edge of second supralabial, passes through nostril, but fails to reach rostral. Anterior nasal in contact with first infralabial and upper edge of second infralabial. Posterior nasal longer than wide, contacting upper margin of second supralabial and preocular. Supralabials four, fourth twice longer than third. Infralabials three, third largest. Eye diameter 0.90 mm; eyes not visible in ventral view, located dorsolaterally, close to suture between preocular and ocular scales, completely covered by ocular scale. Ocular scales contacting frontal. Body cylindrical and robust. Midbody diameter 4.86 mm. Dorsal and ventral scales cycloid, wider than long, highly imbricated and arranged in diagonal series; scale rows around the body 20/20/18. Mid-dorsal scales 215. Ventral scales 211. Cloacal plate rounded, bordered anteriorly by three rows of scales and posteriorly by five rows of scales. Subcaudal scales 11, excluding the terminal spine.

*Skull osteology (*N = 1*; MNRJ 18743):* The length of the skull is 6.52 mm, the width is 2.96 mm. The snout region has a globular enlarged-shape and highly consolidated. The snout articulates with the braincase by the nasal

and prefrontal sutures and with the frontal bone. The anteroventral region of the premaxilla has a short backward process. The midsagittal lamina separates both sides of the premaxilla (Fig. 5). The lamina of the premaxilla is confluent with the mid-dorsal laminae of the nasals and with the mid-dorsal ridges of the vomeronasal cupola of the septomaxillae (Fig. 5). The nasal process of premaxilla contacts the vertical laminae of the nasals in the anterodorsal and posteroventral portions, with the central portion not in contact, leaving a large round canal between the olfactory chambers (Fig. 5A). The medial side of the maxilla has a shallow depression (or fossa), where lodges the maxillary process of the palatine. The palatine fossa is on the lateral side of the maxilla, in the region of the articular fossa. The palatine fossa is large (Fig. 6A), with a diameter of 0.27 mm. The medial border of the maxilla is concave-shaped (Fig. 6C). The ventral pterygoid process of the palatine is straight-shaped and ventrally directed (Fig. 7A). The retroarticular process projects in parallel to the horizontal plane of the articular. The angle between mandibular condyle articulation and the retroarticular process of the compound bone is close to 90° (Fig. 8A). The edentulous dentary is restricted to the distal end of the mandible, articulating mainly with the splenial. The dorsal side of the dentary is flat and pierced by two foramina (Fig. 9A).

*Hemipenial morphology (*N = *4; organs fully everted and inflated):* Hemipenis single, with a long cylindrical body and conical in the distal region (apical cup) (Fig. 13A–D); a tissue sheet extends from the lateral surface of the apical cup, it folds and runs transversely forming a curved papilla (Fig. 13A); the region between this flounce and the lateral sheet is deeper, forming a pocket on the sulcate side (Fig. 13A); internal surfaces of the flounce and the conical termination covered with smooth and shallow striations (Fig. 13A, B); sulcus spermaticus single, protruding over the surface of the hemipenial body, originating on the medial surface of the basal region of the hemipenis and running distally sinuously, reaching the flounce and draining to the pocket of the sulcate side (Fig. 13C); proximal region of the asulcate side of the hemipenial body with a transversal groove (Fig. 13D); medial region of the sulcate and asulcate sides (including the sulcus walls) covered with smooth and shallow striations (Fig. 13C, D).

Coloration of the holotype in preservative: Dorsum (13/11/13 rows scales) pale brown. In the dorsal part of the body up to the tail, a fine darker brown reticulum, particularly concentrated in the central part of dorsal scales (Supporting Information, Fig. S5A). Venter (7/9/5 rows scales) pale cream (Supporting Information, Fig. S5B). Dorsal portions of snout pale cream, with a few

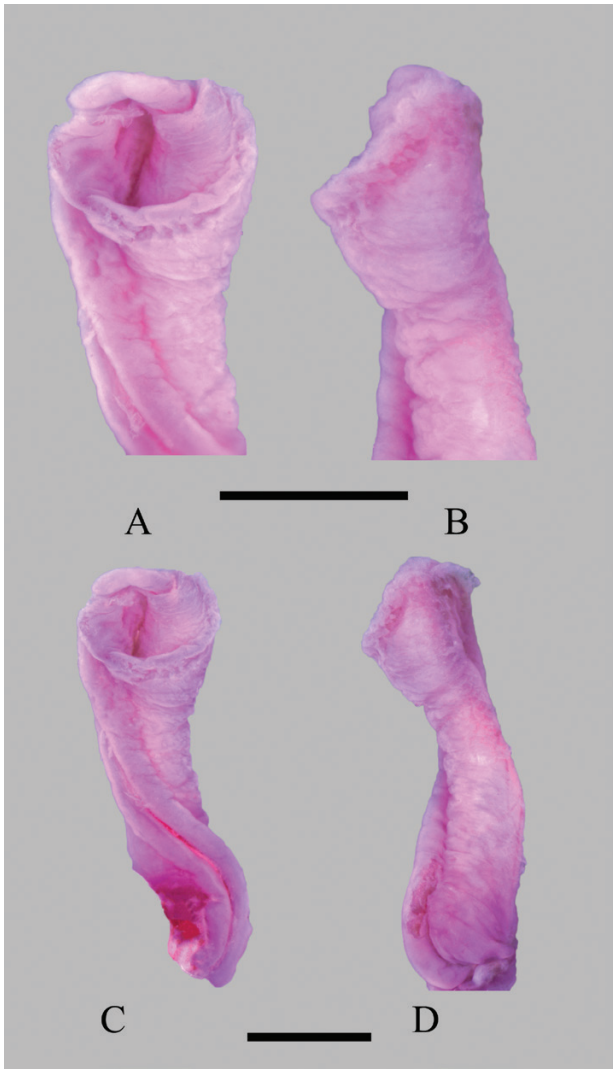

Figure 13. Hemipenis of *Amerotyphlops martis* sp. nov. (MNRJ 18744), detail of the apical region on the sulcate (A) and asulcate views (B), sulcate (C) and asulcate sides (D). Scale bar equal to 1 mm.

light brown spots, covering partially both rostral and nasal scales (Fig. 12A, B). The ventral portion of snout pale cream and immaculate (Fig. 12C). Symphysial region pale cream and immaculate (Fig. 12C). Dorsal head scales (supraoculars, frontal, postfrontal, parietals and occipitals) and dorsal portions of lateral head scales (ocular, nasal and lower nasal) predominantly pale cream with few pale brown spots (Fig. 12A, B) and ventral portions pale cream (Fig. 12C). Cloacal plate pale cream and terminal spine creamy pale brown (Supporting Information, Fig. S5B).

Variation of paratypes: Number of subcaudal scales ten to 12 (mean = 11, SD = 1, *N* = 3). Tail length 2.95–3.20% of TTL (*N* = 3). Largest male with 170 mm TTL.

MBD 4.09–5.13 mm (mean = 4.61, SD = 0.52, *N* = 3); number of mid-dorsal scales 208–217 (mean = 212.3, SD = 4.50, *N* = 3); number of ventral scales 195–208 (mean = 201.0, SD = 6.55, *N* = 3); and number of scale rows around the body 20/20/18 (*N* = 2) or 20/20/20 (*N* = 1). The colour patterns of the paratypes are similar to that found in the holotype (Supporting Information, Fig. S6A–F).

Etymology: The specific epithet is derived from the Latin name '*Mars*', in allusion to the Mars symbol, used to represent the male gender. The choice of the name is a reference to the distinct hemipenial morphology of this species that differs from all other species of *Amerotyphlops*.

Distribution and habitat: Amerotyphlops martis is only known from Praia das Neves, situated at 20 km from the municipality of Presidente Kennedy, state of Espírito Santo, Brazil (Fig. 10B). This region is considered as part of the Atlantic Forest morphoclimatic domain, in the Atlantic Coast Restingas ecoregion, a sandy plain located along to the coast of Brazil (Olson *et al.*, 2001).

The prevalent phytophysiognomy in Praia das Neves is heterogeneous, presenting an herbaceous, shrubs and arboreous forest usually distributed in parallels ridges to the shoreline (Braz *et al.*, 2013), with an annual average of temperature and rainfall of 20 °C and 1561 mm, respectively (Peel *et al.*, 2007). Praia das Neves has several different levels of successional vegetation, with areas close to the beach line presenting herbaceous and shrubby vegetation, with stretches of graminoid beach communities, changing the vegetation in the interior, where presenting a fragmented Ridge forest, with medium height trees (between 15 and 20 m), with lianas, epiphytes and herbaceous understory (Braz *et al.*, 2013).

AMEROTYPHLOPS ILLUSORIUM SP. NOV.

(FIG. 14; SUPPORTING INFORMATION, FIGS S7, S8)

Zoobank registration: urn:lsid:zoobank.org:act:AF7FA356-4412-4C70-AA6D-8C4D24D81966

Holotype: An adult female, MZUSP 18787, (field number MTR 13542), collected by Miguel T. Rodrigues and collaborators on 26 March 2007 from Fazenda Nova Alegria (16° 31′ 50.7″ S, 39° 07′ 06.7″ W, *c.* 30 m a.s.l.), municipality of Trancoso, state of Bahia, Brazil (Fig. 14; Supporting Information, Fig. S7).

Paratypes: Two male specimens, MNRJ 19614 and MNRJ 19613, collected by Tiago S. Soares between 6 and 15 June 2010 from Praia de Porto Seguro, municipality of Trancoso, state of Bahia, Brazil (Supporting Information, Fig. S8A–D).

Diagnosis: This species is distinguished from all other South American congeneric species by the unique combination of the following of characters: (1) nasal suture incomplete; (2) rostral scale oval; (3) supralabial scales four; (4) infralabial scales three; (5) rows scales around the body 20/20/18; (6) mid-dorsal scales 221–230; (7) ventral scales 210–219; (8) rows of dorsal scales dark brown 13–15; (9) rows of ventral

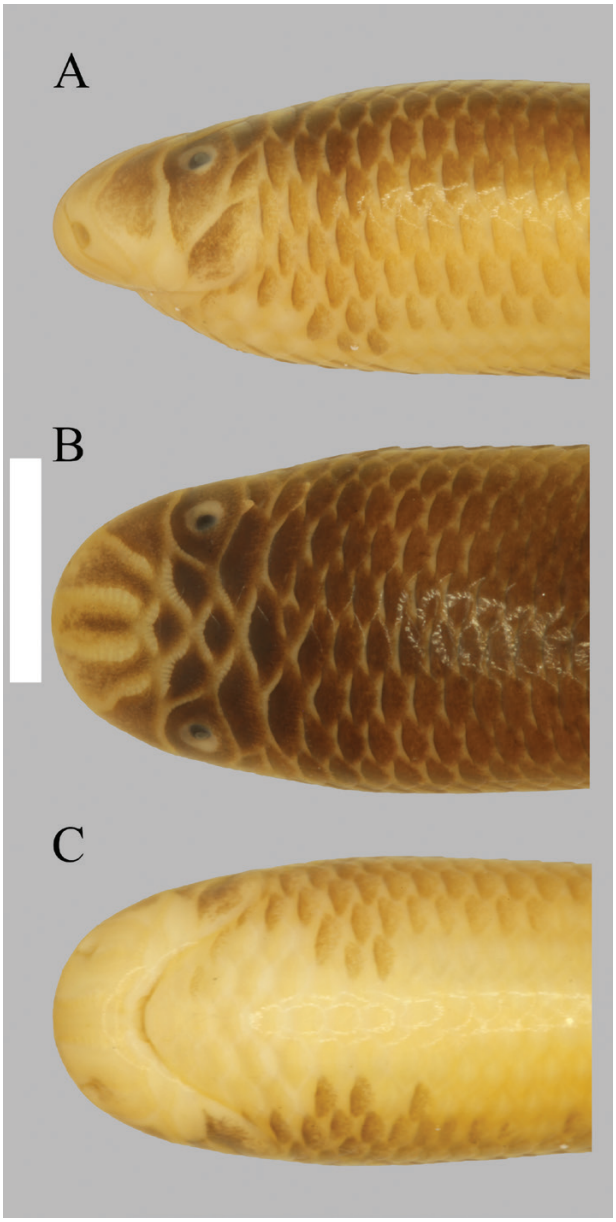

Figure 14. Holotype of *Amerotyphlops illusorium* sp. nov. (MZUSP 18787). Head in left lateral (A), dorsal (B) and ventral (C) views. TTL = 229 mm. Scale bar equal to 5 mm.

scales yellowish cream and immaculate five to seven; (10) caudal spine dark brown; (11) subcaudal scales ten to 12; (12) maximum TTL 229 mm; (13) maximum TL 6 mm; (14) nasal process of premaxilla contacting the vertical laminae of the nasals in the anterodorsal and posteroventral portions, with the central portion not in contact, leaving a large round canal between the olfactory chambers; (15) large palatine fossa on the lateral side of the maxilla; (16) maxilla with a straight medial border; (17) ventral pterygoid process of palatine straight; (18) ratio between length of ventral pterygoid process of palatine and skull length 0.06; (19) angle between mandibular condyle articulation and the retroarticular process of the compound bone close to 90°; and (20) dorsal surface of dentary bone with one to two evident foramina.

Amerotyphlops illusorium differs from *A. costaricensis*, *A. lehneri*, *A. microstomus*, *A. stadelmani*, *A. tasymicris*, *A. tenuis*, *A. trinitatus* and *A. tycherus* by having an incomplete nasal suture (vs. complete nasal suture); from *A. arenensis*, *A. caetanoi*, *A. amoipira*, *A. minuisquamus*, *A. paucisquamus* and *A. yonenagae* by having 20/20/18 rows scales around the body (vs. 18/16/14, 18/18/14, 20/18/14 or 20/18/15 in *A. minuisquamus* and 18/18/18 in *A. arenensis*, *A. caetanoi*, *A. amoipira*, *A. paucisquamus* and *A. yonenagae*); from *A. reticulatus* by having highly pigmented cephalic scales with a dark brown dorsum and dorsum tail brown (vs. yellow and few pigmented cephalic scales, dorsum brown or black and dorsum tail black with cream or yellow spot); from *A. montanum* by having a smaller rostral width (RW1) at the dorsal portion, between 1.22 and 1.54 mm (vs. a larger rostral width at the dorsal portion 1.88 mm); from *A. martis* by having a largest number of mid-dorsal scales, between 221 and 230 (vs. fewer number of mid-dorsal scales, between 208 and 217); and from *A. brongermianus* by having the ventral portion of the pterygoid process of palatine straight (vs. ventral pterygoid process of palatine curved). Table 1 shows additional morphometric characters and scale patterns found in *A. illusorium* and morphologically similar species distributed in southern and north-eastern Brazil.

Description of the holotype: Adult female, TTL 229 mm, TL 6 mm, MBD/(SVL-HR) 0.037 mm and TL/SVL 37.16 mm. Head slightly depressed dorsoventrally, not wider than 'neck'. Snout round in dorsal and ventral views. Rostral oval, longer than wide, narrow at anteroposterior region and wider at medial region; visible in dorsal view, extending ventrodorsally without reaching the imaginary transverse line between anterior borders of eyes. Rostral contacting nasal (anterior and posterior) dorsolaterally and first supralabial and anterior nasal scales ventrally. Nasal suture incomplete, only partially dividing the anterior and posterior portions of nasal scale. Suture begins in the upper edge of second supralabial, passes through nostril, but fails to reach rostral. Anterior nasal in contact with first infralabial and upper edge of second infralabial. Posterior nasal longer than wide, contacting upper margin of second supralabial and preocular. Supralabials four, fourth twice longer than third. Infralabials three, third largest. Eye diameter 0.77 mm; eyes not visible in ventral view, located dorsolaterally, close to suture between preocular and ocular scales, completely covered by ocular scale. Ocular scales contacting frontal. Body cylindrical and robust. Midbody diameter 8.28 mm. Dorsal and ventral scales cycloid, wider than long, highly imbricated and arranged in diagonal series; scale rows around the body 20/20/18. Mid-dorsal scales 221. Ventral scales 218. Cloacal plate rounded, bordered anteriorly by three rows of scales and posteriorly by five rows of scales. Subcaudal scales ten, excluding the terminal spine. Terminal spine large, stout base and dark brown.

*Skull osteology (*N = *2; MZUSP 18787 and MNRJ 19613):* Length of the skull 7.03–8.22 mm, and skull width 3.46–3.99 mm. The snout region has a globular enlarged-shape and highly consolidated. The snout articulates with the braincase by the nasal and prefrontal sutures and with the frontal bone. The anteroventral region of the premaxilla has a short backward process. The midsagittal lamina separates both sides of the premaxilla (Fig. 5). The lamina of the premaxilla is confluent with the mid-dorsal laminae of the nasals and with the mid-dorsal ridges of the vomeronasal cupola of the septomaxillae (Fig. 5). The nasal process of premaxilla contacting the vertical laminae of the nasals in the anterodorsal and posteroventral portions, with the central portion not in contact, leaving a large round canal between the olfactory chambers (Fig. 5A). The medial side of the maxilla has a shallow depression (or fossa), where lodges the maxillary process of the palatine. The palatine fossa is on the lateral side of the maxilla, in the region of the articular fossa. The palatine fossa is large (Fig. 6A), with diameters between 0.24 and 0.29 mm long. The medial border of the maxilla is straight-shaped (Fig. 6A). The pterygoid process of the palatine is straight-shaped and ventrally directed (Fig. 7A). The retroarticular process projects in parallel to the horizontal plane of the articular. The angle between mandibular condyle articulation and the retroarticular process of the compound bone is close to 90° (Fig. 8A). The edentulous dentary is restricted to the distal end of the mandible,

articulating mainly with the splenial. The dorsal side of the dentary is flat and pierced by one or two foramina (Fig. 9A).

Coloration of the holotype in preservative: Dorsum (13/13/13 rows scales) dark brown, venter (7/7/5 rows scales) yellowish cream (Fig. S7A, B). Dorsal portions of snout yellowish cream, with a dark brown spot, covering both rostral and nasal scales (Fig. 14A, B). Ventral portion of snout yellowish cream and immaculate (Fig. 14C). Symphysial region yellowish cream and immaculate (Fig. 14C). Dorsal head scales (supraoculars, frontal, postfrontal, parietals and occipitals) and dorsal portions of lateral head scales (ocular, nasal, and lower nasal) predominantly dark brown (Fig. 14A, B) and ventral portions yellowish cream (Fig. 14C). Cloacal plate pale yellowish cream and terminal spine dark brown (Fig. S7B).

Variation of paratypes: Number of subcaudal scales 11–12 (mean = 11.5, SD = 0.7, $N = 2$). Tail length 2.58–3.0 % of TTL ($N = 2$). Largest male with 207 mm TTL. MBD 4.91–5.11 mm (mean = 5.01, SD = 0.13, $N = 2$); number of mid-dorsal scales 226–230 (mean = 228.0, SD = 2.82, $N = 2$); number of ventral scales 210–219 (mean = 214.0, SD = 6.36, $N = 2$); and number of scale rows around the body 20/20/18. The colour patterns of the paratypes are similar to that found in the holotype (Supporting Information, Fig. S8A–D).

Etymology: The specific epithet is derived from the Latin adjective *illusorius*, illusory or ironic, in reference to the external morphology that challenges its identification when compared to *Amerotyphlops brongersmianus*.

Distribution and habitat: Amerotyphlops illusorium is known from Fazenda Nova Alegria, situated at 6 km from the municipality of Trancoso, in the state of Bahia, Brazil (Fig. 10B). This region is considered as part of the Atlantic Forest morphoclimatic domain, in the Bahia Coastal forest ecoregion, along the north-eastern coast of Brazil (Olson *et al.*, 2001)

The prevalent phytophysiognomy in Trancoso presenting a restinga and ombrophilous dense lowland forests (Veloso *et al.*, 1991; Rizzini, 1997; Assis *et al.*, 2011), with an elevational gradient ranging from sea level to 50 m a.s.l., with an annual average of temperature of 24.4 °C and rainfall between 1300 and 1600 mm, respectively (Veloso *et al.*, 1991; Rizzini, 1997; Assis *et al.*, 2011; Santos, 2013). This region has several different levels of successional vegetation, with areas close to the sandplain with herbaceous, shrubs and arboreous forest and areas at the beginning of piedmont, with lowland forests, with medium height trees (approximately 20 m), with epiphytes and herbaceous understory (Santos, 2013).

DISCUSSION

Diversity of South American *Amerotyphlops* Hedges *et al.*, 2014

Regardless of the recent advances in our knowledge about the diversity of South American blind snakes the genus *Amerotyphlops* remains elusive, with several species still known only from their type series (Graboski *et al.*, 2015, 2018). Our molecular and morphological analyses revealed four new species of *Amerotyphlops*, distributed throughout the north-eastern and south-eastern parts of the Brazilian Atlantic rain forest (ARF), representing an increase of 50% in the diversity of this group. *Amerotyphlops illusorium*, *A. martis* and *A. montanum* occur sympatrically and are morphologically similar to *A. brongersmianus*, while *A. caetanoi* is morphologically similar to *A. arenensis* and is sympatric with *A. amoipira*, *A. arenensis* and *A. yonenagae* (Fig. 10A, B).

The ARF is among the most biodiverse regions in the world, containing a high number of endemic and threatened species (Myers *et al.*, 2000). This biome comprises different types of vegetation or forest formations distributed in both tropical and subtropical areas (Scarano, 2006; Marques *et al.*, 2011; IBGE, 2012). In the last decade, many studies supported the existence of biogeographical barriers (e.g. rivers or mountains) defining areas with high levels of biodiversity and diversification within the ARF (Thomas *et al.*, 1998; Costa, 2003; Pellegrino *et al.*, 2005; Cabanne *et al.*, 2007; Carnaval *et al.*, 2009, 2014; Lirio *et al.*, 2015; Barbo *et al.*, 2022a). However, several studies have suggested that ecological factors (e.g. climate, soil and disturbance) may also be responsible for these geographically restricted areas of high endemism (Rocha *et al.*, 2005; Grazziotin *et al.*, 2006; Rocha & Sluys, 2007; Thomé *et al.*, 2010; Carnaval *et al.*, 2014; Saiter *et al.*, 2016).

Saiter *et al.* (2016) divided the ARF into three major subregions based on floristic composition: (1) Bahia interior forests, encompassing moist and dry forests throughout the interior lands of the state of Bahia and north-eastern Minas Gerais; (2) Bahia coastal forests, encompassing the wet forests of the northern extreme of the state of Espírito Santo and most of the coastal region of Bahia; and (3) Krenák-Waitaká, which encompasses the wet forests of southern Espírito Santo. Furthermore, Rocha *et al.* (2005) analysed the status of endemic and endangered terrestrial vertebrates inhabiting the coastal sandplains (Restingas) along the eastern coast of Brazil, and identified three main

areas of high endemism: (1) the coastal Restingas stretching from northern Espírito Santo to southern Bahia; (2) the coastal Restingas encompassing the regions of Maricá and Jurubatiba in the state of Rio de Janeiro state; and (3) Praia das Neves in the southern part of the state of Espírito Santo.

The Restingas and Bahia coastal and interior forests have been shown as highly biodiverse areas in the ARF, with the incidence of endemic and threatened species for several groups of organisms (Rocha *et al.*, 2005, 2007; Silva & Satyamurty, 2006; Carnaval *et al.*, 2009; Mattos *et al.*, 2009; Telles *et al.*, 2012; Cosendey *et al.*, 2016; Saiter *et al.*, 2016; Medina *et al.*, 2020). All new species of *Amerotyphlops* described in the present study are endemic to these areas: *Amerotyphlops illusorium* and *A. martis* are restricted to ombrophilous dense lowland coastal forests of Bahia and the Restingas of Espírito Santo, while *A. montanum* and *A. caetanoi* occur in the ombrophilous dense and semi-deciduous coastal forests and submontane seasonal semi-deciduous forests of the interior of Bahia, respectively (Rodrigues *et al.*, 2002, 2013; Recoder *et al.*, 2010).

Comparative hemipenial morphology of South American *Amerotyphlops*

Hemipenes of South American *Amerotyphlops* follow the general pattern observed in scolecophidians, with single organs with an undivided sulcus spermaticus (Branch, 1986; Wallach, 1998; Graboski *et al.*, 2018). Recently, Montingelli et al. (2022) demonstrated that the hemipenes of scolecophidians retain a plesiomorphic lizard condition. *Amerotyphlops martis* also conforms to this general morphology, with a sulcus spermaticus that flares near the tip of an expanded apical cup (Montingelli et al., 2022). The organs of *A. minuisquamus* and *A. reticulatus* are unique in presenting large and calcified spines, while this character is absent in other species of *Amerotyphlops* (Dixon & Hendricks, 1979; Graboski *et al.*, 2018; Montingelli et al., 2022). The hemipenis of *Amerotyphlops martis* is similar to *A. brongersmianus*, differing only by the presence of an additional structure in the apical cup. According to our results and previous studies (Graboski *et al.*, 2018), the micro- and macro-ornamentation was shown to be highly diverse and taxonomically informative, representing a potential source of characters that can be used to differentiate and describe hidden diversity.

Comparative osteological morphology of South American *Amerotyphlops*

Traditionally in taxonomic and systematics studies, osteological characters have been obtained from a variety of invasive methodologies, which considerably reduced the availability of specimens and their representation in these studies (Cundall & Irish, 2008; Bell & Mead, 2014; Bell *et al.*, 2021). Additionally, the interpretation of the osteological character and its variation in scolecophidians has been controversial in taxonomic studies, since osteological descriptions for most taxa have been based on single-specimen preparations (List, 1966; Bell & Mead, 2014). The sample size of the four species described here is a direct product of the scarcity of specimens collected during fieldwork expeditions and their rarity in the natural history collection, which is typical in most studies involving South American scolecophidians (Rodrigues, 1991; Rodrigues & Juncá, 2002; Graboski *et al.*, 2015).

The use of non-invasive methodologies (e.g. HRXCT) in the description and evaluation of osteology has granted access to data from taxa represented by a single or just a few specimens stored in natural history museums (Bell & Mead, 2014; Bell *et al.*, 2021). The lack of large samples of osteological preparations can hinder the recognition of the unique patterns of variation required in taxonomic studies. However, the skull osteology of the four new species described here was obtained by HRXCT, which allowed us to recognize discrete and continuous characters from concealed portions of the internal anatomy of the skull (see characters 14 to 20 in each species diagnosis and Table S4).

Postnatal allometric growth is a common trait through most bone structures in squamates (Rossman, 1980; Scanferla & Bhullar, 2014; Palci *et al.*, 2016), and its variation (mainly in size and sturdiness) in skulls of scolecophidians has been attributed to differences in age and body size (Laver *et al.*, 2021). Based on our osteological samples, we did not recognize size-dependent variation associated with ontogeny. Also, our set of osteological diagnostic characters exhibited no variation associated with skull size (see diagnostic characters for each species and Supporting Information, Table S2), except for the continuous diagnostic characters (15, 18 and 19), which showed distinctive allometric patterns for each species. For example, *Amerotyphlops montanum* has a medium-sized skull (SL = 8.08 mm) but a small palatine fossa (PFD = 0.17 mm), while *A. caetanoi* has a small skull (SL = 6.15 mm) and a large palatine fossa (PFD = 0.25 mm) (Fig. 6).

In scolecophidians, females usually have a larger body and head size than males (Cox *et al.*, 2007). However, few studies have explored the relationship between skeletal anatomy variation and sexual dimorphism. Pinto *et al.* (2015) studied the sexual dimorphism in *Trilepida salgueroi* (Amaral, 1955) and found differences between males and females in the size and number of thoracolumbar

and caudal vertebrae. In our osteological analysis we did not recognize sexual-dependent variation associated with dimorphism (e.g. *A. brongersmianus* and *A. illusorium*; see Supporting Information, Table S5).

After six decades of List's (1966) primal study – one of the most complete studies on typhlopoid and leptotyphlopoid skull osteology – the amount of knowledge on osteology of scolecophidians is still elusive. However, our current results agree with McDowell's (1967) suggestion that osteological characters are valuable sources of evidence to evaluate the taxonomy of scolecophidians and to support the definition of natural groups. Although we acknowledge that the anatomy of the skull of *Amerotyphlops* remains poorly studied (List, 1966; Lira & Martins, 2021), the set of information presented here indicates a broad osteological variation for the genus. We expect that further studies on the skull morphology of *Amerotyphlops* will shed light on different evolutionary aspects of anatomy, ecology, behaviour and diversification patterns of this elusive lineage of fossorial snakes.

Cryptic species and morphological variation

Studies about genetic variability have been shown to be essential in assessing and inferring the cryptic diversity of all sorts of organisms (Daly & Patton, 1990; O'Connell *et al.*, 2021). Studies based on DNA evidence have shown that some fossorial vertebrates have highly diversified modes of speciation, ranging from rapid and almost sympatric chromosomal speciation (Reig *et al.*, 1990; Massarini *et al.*, 2002) to allopatric speciation by geographic isolation (Daly & Patton, 1990; Steinberg *et al.*, 2000; Maddock *et al.*, 2020; O'Connell *et al.*, 2021). The study of Thomas & Hedges (2007) represents a noteworthy example with scolecophidians, in which genetic information helped them to focus their attention on morphological traits capable of diagnosing hidden diversity. Based on genetic and morphological evidence, they described 11 cryptic species of *Typhlops* from Hispaniola, some of which were sympatric and almost indistinct from other species (Thomas & Hedges 2007).

Our results corroborate the validity of the Thomas & Hedges (2007) approach for scolecophidians. The phylogenetic information generated based on DNA sequences provided us with a solid framework on which to base our search for variability in morphological characters. Most of the external morphology (e.g. pholidosis) does not differentiate the new species described here from the widespread species *A. brongersmianus*, indicating their cryptic nature. However, we were able to include quantitative morphometric traits and qualitative hemipenial and skull osteology characters that enabled us to delimit these four highly divergent molecular lineages of *Amerotyphlops* as new species.

Extreme environmental conditions can impose stabilization on phenotypic characteristics (Lefébure *et al.*, 2006; Bickford *et al.*, 2007). These environments are characterized by the presence of physicochemical stressors that are lethal to most organisms (Wharton, 2002; Bell, 2012; Riesch *et al.*, 2015; Tobler *et al.*, 2018). Fossorial organisms, like blind snakes and rodents, must be adapted to the extreme hypoxia and hypercapnia found in their burrows as a consequence of oxygen consumption and low gas-permeability of the soil (McNab, 1966). An emblematic case is the subterranean amphipod *Niphagus virei* Chevreux, 1896 complex that occupies habitats marked by a complete lack of light and long periods of anoxia and food shortages (Malard & Hervant, 1999; Hüppop, 2000; Lefébure *et al.*, 2006). In this case, molecular analyses indicated three highly divergent clades (over 13 million years of divergence), but no specific morphological character can differentiate individuals belonging to these highly divergent clades. These studies reinforce the idea that an organism with an underground lifestyle may have selective restrictions for adapting to extreme conditions, which certainly limit morphological variation (Nevo,

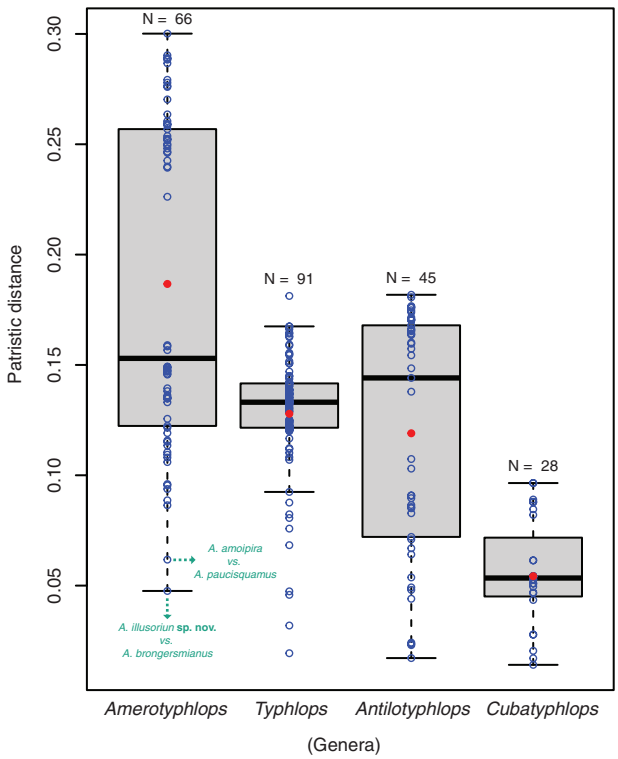

Figure 15. Boxplot of patristic distance among Typhlopinae (*Amerotyphlops*, *Typhlops*, *Antilotyphlops* and *Cubatyphlops*).

1979). The results of our morphological analyses support these studies, indicating, overall, a low level of morphological dissimilarity among species of *Amerotyphlops*. Particularly, the distribution of the morphological diversity in the multivariate space indicates extensive overlap between *A. illusorium* and *A. brongersmianus*, and a slight overlap between *A. montanum* and *A. brongersmianus*. However, our molecular phylogenetic analysis showed that all four new species represent independent lineages and exhibit high levels of genetic distances among them. Although *A. illusorium* and *A. brongersmianus* showed the lowest patristic distances within the genus (Fig. 15), the amplitude of the interspecific distance was higher than that found among species of other genera of Typhlopinae (e.g. *Antillotyphlops* and *Cubatyphlops*) (Fig. 15). Our study strongly indicates that an integrative approach is essential to evaluate the diversity of poorly studied groups of fossorial organisms, such as blind snakes, which tend to present highly conservative morphologies.

Conservation status

Although the description of four new species increases the diversity and our knowledge of South American *Amerotyphlops*, these snakes are still considered rare and elusive. The most recent list of Brazilian endangered species (https://www.icmbio.gov.br/portal_antigo/biodiversidade/fauna-brasileira/lista-de-especies.html) included *A. amoipira* and *A. yonenagae* in the category of endangered (EN), while *A. paucisquamus* is in the category of vulnerable (VU). Therefore, these species are currently considered under threat due to their restricted distribution and scarcity.

The four new species described here are also known only from their type locality in the Brazilian Atlantic rain forest, one of the most impacted Brazilian biomes (SOS Mata Atlântica & Instituto Nacional de Pesquisas Espaciais, 2000; Silva *et al.*, 2007; Ribeiro *et al.*, 2009). The description of these species reinforces the importance of conservation policies towards the north-eastern remnants of the ARF, as well as their coastal sandplain ecoregion known as Restingas.

CONCLUSIONS

Despite recent advances in the higher level systematics of scolecophidians, the diversity of this elusive group of snakes remains poorly evaluated in South America. Our study explored, through integrative analytic approaches based on an expanded taxon sampling, the cryptic nature of the South American blind snakes, genus *Amerotyphlops*, showing that their diversity has been largely underestimated.

ACKNOWLEDGEMENTS

The authors thank the following colleagues who supplied tissue samples and specimens loans for the present study: Antônio Argôlo (UESC), Paulo Roberto Manzani and Luis Felipe de Toledo Ramos Pereira (ZUEC), Paulo Passos (MNRJ), Santiago Castroviejo-Fisher and Glaucia F. Pontes (MCP-PUCRS), Frederico França and Gustavo Vieira (UFPB), Renato Feio (MZUFV), Felipe Franco Curcio (UFMT), Fernanda Werneck (INPA), Daniel Loebman (FURG), Selma Torquato (MUFAL), Gilda Andrade (UFMA), Róbson Ávila (URCA), Rejâne Lira da Silva (UFBA), Robert Murphy (ROM), Adrian Garda (UFRN), João Tonini, Gindomar Gomes Santana, Gentil Pereira Filho and Marco Antônio de Freitas. We also thank Rosely Rodrigues da Silva, Alberto Barbosa de Carvalho and Jaqueline Battilana from MZUSP for technical support.

RG was supported by a scholarship from Fundação de Amparo à Pesquisa do Estado de São Paulo scholarship (FAPESP, 2008/52285-0) and Programa de Capacitação Institucional (MPEG-MCTI, 301346/2020-8). JCA was supported by a scholarship from the Coordenação de Aperfeiçoamento de Pessoal de Nível Superior (CAPES). FGG was supported by Fundação de Amparo à Pesquisa do Estado de São Paulo (FAPESP, 2012/08661-3 and 2016/13469-5) and Conselho Nacional de Desenvolvimento Científico e Tecnológico (CNPq, 312016/2021-2). RAGF was supported by a grant from Apoio Estratégico a Projetos Emergentes da Universidade Federal do Pará (PAEPE-UFPA; 23073.020915/2020-35). ALCP thanks Conselho Nacional de Desenvolvimento Científico e Tecnológico (CNPq, 30.2611/2018-5 and 44.462/2020). SLB thanks Conselho Nacional de Desenvolvimento Científico e Tecnológico (CNPq, 310472/2017-2) for support. MTR thanks Fundação de Amparo à Pesquisa do Estado de São Paulo (FAPESP, 2003/10335-8 and 2011/501-46), Conselho Nacional de Desenvolvimento Científico e Tecnológico (CNPq) and the students of his lab for help in the field. This research was supported through grants from Fundação de Amparo à Pesquisa do Estado de São Paulo (FAPESP, 2011/50206-9 and 2016/50127-5) to HZ.

CONFLICTS OF INTEREST

The authors declare no conflict of interest.

DATA AVAILABILITY

DNA sequences generated in this study are deposited in the GenBank Nucleotide Database and can be accessed with unique accession numbers that are given

within this publication and in Supporting Information, Table S3. All other data generated or analyzed during this study are included in this published article and its supplementary information files. Scripts used in our morphological analyses are available from the Figshare repository (https://doi.org/10.6084/m9.figshare.20092721).

REFERENCES

Adalsteinsson SA, **Branch WR**, **Trape S**, **Vitt LJ**, **Hedges SB. 2009.** Molecular phylogeny, classification, and biogeography of snakes of the family Leptotyphlopidae (Reptilia, Squamata). *Zootaxa* **2244:** 1–50.

Amaral A. 1955. Contribuição ao conhecimento dos ofídios neotropicos: 14. Descricao de duas especies novas de "cobra-cega" (fam. Leptotyphlopidae). *Memórias do Instituto Butantan* **26:** 203–205.

Amorim AM, **Matos FB. 2009.** A vegetação do complexo de Serra das Lontras. In: SAVE Brasil, IESB, BirdLife, eds. *Complexo de Serras das Lontras e Una, Bahia: elementos naturais e aspectos de sua conservação*. São Paulo: SAVE Brasil, 16–25.

de Arruda MP, **Almeida CHLN**, **Rolim DC**, **Maffei F. 2011.** First record in midwestern region of the state of São Paulo, Brazil of *Typhlops brongersmianus* Vanzolini, 1976 (Squamata: Typhlopidae). *Check List* **7:** 571–573. Doi: 10.15560/7.4.571.

Assis MA, **Prata EMB**, **Pedroni F**, **Sanchez M**, **Eisenlohr PV**, **Martins FR**, **Santos FAM**, **Tamashiro JY**, **Alves LF**, **Vieira SA**, **Piccolo MC**, **Martins SC**, **Camargo PB**, **Carmo JB**, **Simões E**, **Martinelli LA**, **Joly CA. 2011.** Florestas de restinga e de terras baixas na planície costeira do sudeste do Brasil: vegetação e heterogeneidade ambiental. *Biota Neotropica* **11:** 103–121. Doi: 10.1590/S1676-06032011000200012.

Barbo FE, **Grazziotin FG**, **Pereira-Filho GA**, **Freitas MA**, **Abrantes SH**, **Kokubum MNDC. 2022a.** Isolated by dry lands: integrative analyses unveil the existence of a new species and a previously unknown evolutionary lineage of Brazilian lanceheads (Serpentes: Viperidae: *Bothrops*) from a Caatinga moist-forest enclave. *Canadian Journal of Zoology* **100:** 147–159. Doi: 10.1139/cjz-2021-0131.

Barbo FE, **Booker WW**, **Duarte MR**, **Chaluppe B**, **Portes-Junior JA**, **Franco FL**, **Grazziotin FG. 2022b.** Speciation process on Brazilian continental islands, with the description of a new insular lancehead of the genus *Bothrops* (Serpentes, Viperidae). *Systematics and Biodiversity* **20:** 1–25. Doi: 10.1080/14772000.2021.2017059.

Barbour T. 1914. A contribution to the zoögeography of the West Indies, with special reference to amphibians and reptiles. *Memoirs of the Museum of Comparative Zoölogy* **44:** 205–359.

Bell EM. 2012. *Life at extremes: environments, organisms and strategies for survival*. Wallingford: CABI. Doi: 10.1079/9781845938147.0000.

Bell CJ, **Mead JI. 2014.** Not enough skeletons in the closet: collections-based anatomical research in an age of conservation conscience. *The Anatomical Record* **297:** 344–348. Doi: 10.1002/ar.22852.

Bell CJ, **Daza JD**, **Stanley EL**, **Laver RJ. 2021.** Unveiling the elusive: X-rays bring scolecophidian snakes out of the dark. *The Anatomical Record* **304:** 2110–2117. Doi: 10.1002/ar.24729.

Bickford D, **Lohman DJ**, **Sodhi NS**, **Nvjot PKL**, **Meier R**, **Winker K**, **Ingram KK**, **Das I. 2007.** Cryptic species as a window on diversity and conservation. *Trends in Ecology & Evolution* **22:** 148–155. Doi: 10.1016/j.tree.2006.11.004.

Branch WR. 1986. Hemipenial morphology of African snakes: a taxonomic review. Part 1. Scolecophidia and Boidae. *Journal of Herpetology* **20:** 285–299. Doi: 10.2307/1564495.

Braz DM, **Jacques EL**, **Somner GV**, **Sylvestre LS**, **Rosa MMT**, **Pereira-Moura MVL**, **Germano Filho P**, **Couto AVS**, **Amorim TA. 2013.** Restinga de Praia das Neves, ES, Brasil: caracterização fitofisionômica, florística e conservação. *Biota Neotropica* **13:** 315–331. Doi: 10.1590/S1676-06032013000300032.

de Brito PS, **Freire EMX. 2012.** New records and geographic distribution map of *Typhlops amoipira* Rodrigues and Juncá, 2002 (Typhlopidae) in the Brazilian rainforest. *Check List* **8:** 1347–1349. Doi: 10.15560/8.6.1347.

Cabanne GS, **Santos FR**, **Miyaki CY. 2007.** Phylogeography of *Xiphorhynchus fuscus* (Passeriformes, Dendrocolaptidae): vicariance and recent demographic expansion in southern Atlantic forest. *Biological Journal of the Linnean Society* **91:** 73–84. Doi: 10.1111/j.1095-8312.2007.00775.x.

Caicedo-Portilla JR. 2011. Dimorfismo sexual y variación geográfica de la serpiente ciega *Typhlops reticulatus* (Scolecophidia: Typhlopidae) y distribución de otras especies del género en colombia. *Caldasia* **33:** 221–234.

Carnaval AC, **Hickerson MJ**, **Haddad CFB**, **Rodrigues MT**, **Moritz C. 2009.** Stability predicts genetic diversity in the Brazilian Atlantic forest hotspot. *Science* **323:** 785–789. Doi: 10.1126/science.1166955.

Carnaval AC, **Waltari E**, **Rodrigues MT**, **Rosauer D**, **VanDerWal J**, **Damasceno R**, **Prates I**, **Strangas M**, **Spanos Z**, **Rivera D**, **Pie MR**, **Firkowski CR**, **Bornschein MR**, **Ribeiro LF**, **Moritz C. 2014.** Prediction of phylogeographic endemism in an environmentally complex biome. *Proceedings of the Royal Society B: Biological Sciences* **281:** 20141461. Doi: 10.1098/rspb.2014.1461.

Chretien J, **Wang-Claypool CY**, **Glaw F**, **Scherz MD. 2019.** The bizarre skull of *Xenotyphlops* sheds light on synapomorphies of Typhlopoidea. *Journal of Anatomy* **234:** 637–655. Doi: 10.1111/joa.12952.

Cignoni P, **Callieri M**, **Corsini M**, **Dellepiane M**, **Ganovelli F**, **Ranzuglia G. 2008.** *Meshlab: an open-source mesh processing tool*. Eurographics Italian Chapter Conference, Salerno, Italy, 129–136.

Cope ED. 1866. Fourth contribution to the herpetology of tropical America. *Proceedings of the Academy of Natural Sciences of Philadelphia* **18:** 123–132.

Correia LL, **Nunes PMS**, **Gamble T**, **Maciel AO**, **Marques-Souza S**, **Fouquet A**, **Rodrigues MT**, **Mott T. 2018.** A new species of *Brasilotyphlus* (Gymnophiona: Siphonopidae) and a contribution to the knowledge of the relationship between *Microcaecilia* and *Brasilotyphlus*. *Zootaxa* **4527:** 186–196. Doi: 10.11646/zootaxa.4527.2.2.

Cosendey BN, **Rocha CFD**, **de Menezes VA. 2016.** Population density and conservation status of the teiid lizard *Cnemidophorus littoralis*, an endangered species endemic to the sandy coastal plains (restinga habitats) of Rio de Janeiro state, Brazil. *Journal of Coastal Conservation* **20:** 97–106. Doi: 10.1007/s11852-016-0421-4.

Costa LP. 2003. The historical bridge between the Amazon and the Atlantic forest of Brazil: a study of molecular phylogeography with small mammals. *Journal of Biogeography* **30:** 71–86. Doi: 10.1046/j.1365-2699.2003.00792.x.

Couto APL, **Funch LS**, **Conceição AA. 2011.** Composição florística e fisionomia de floresta estacional semidecídua submontana na Chapada Diamantina, Bahia, Brasil. *Rodriguésia* **62:** 391–405. Doi: 10.1590/2175-7860201162213.

Cox RM, **Butler MA**, **John-Alder HB. 2007.** The evolution of sexual size dimorphism in reptiles. In: Fairbairn DJ, Blanckenhorn WU, Székely T, eds. *Sex, size and gender roles: evolutionary studies of sexual size dimorphism*. Oxford: Oxford University Press, 38–49. Doi: 10.1093/acprof:oso/9780199208784.003.0005.

Cundall D, **Irish F. 2008.** The snake skull. In: Gans C, Gaunt AS, Adler K, eds. *Biology of the Reptilia. The skull of Lepidosauria*. Salt Lake City: Society for the Study of Amphibians and Reptiles, 349–392.

Daly JC, **Patton JL. 1990.** Dispersal, gene flow, and allelic diversity between local populations of *Thomomys bottae* pocket gophers in the coastal ranges of California. *Evolution* **44:** 1283–1294. Doi: 10.1111/j.1558-5646.1990.tb05232.x.

Daniels SR, **Heideman NJL**, **Hendricks MGJ. 2009.** Examination of evolutionary relationships in the Cape fossorial skink species complex (Acontinae: *Acontias meleagris meleagris*) reveals the presence of five cryptic lineages. *Zoologica Scripta* **38:** 449–463. Doi: 10.1111/j.1463-6409.2009.00387.x.

Davis JI, **Nixon KC. 1992.** Populations, genetic variation, and the delimitation of phylogenetic species. *Systematic Biology* **41:** 421–435. Doi: 10.1093/sysbio/41.4.421.

Dixon JR, **Hendricks FS. 1979.** The wormsnakes (Family Typhlopidae) of the Neotropics, exclusive of the Antilles. *Zoologische Verhandelingen* **173:** 1–39.

Duméril AMC, **Bibron G. 1844.** *Erpetologie Générale ou Histoire Naturelle Complete des Reptiles. Tome 6*. Paris: Librairie Encyclopédique Roret, 609.

Esri. 1999. *ArcGIS (version 10.2.2) Environmental Systems*. New York: Research Institute Inc.

Fernández-Stolz GP, **Stolz JFB**, **de Freitas TRO. 2007.** Bottlenecks and dispersal in the Tuco-Tuco Das Dunas, *Ctenomys flamarioni* (Rodentia: Ctenomyidae), in southern Brazil. *Journal of Mammalogy* **88:** 935–945. Doi: 10.1644/06-MAMM-A-210R1.1.

Fišer C, **Robinson CT**, **Malard F. 2018.** Cryptic species as a window into the paradigm shift of the species concept. *Molecular Ecology* **27:** 613–635. Doi: 10.1111/mec.14486.

Fox J, **Weisberg S. 2019.** *An R companion to applied regression*. Thousand Oaks: Sage.

de França RC, **Germano CE de S**, **França FGR. 2012.** Composition of a snake assemblage inhabiting an urbanized area in the Atlantic forest of Paraíba State, northeast Brazil. *Biota Neotropica* **12:** 1–13.

de Freitas MA, **Silva TFS**, **Fonseca PM**, **Hamdan B**, **Filadelfo T**, **Abegg AD. 2019.** Herpetofauna of Serra do Timbó, an Atlantic forest remnant in Bahia State, northeastern Brazil. *Herpetology Notes* **12:** 245–260.

Frost D. 2018. *Amphibian species of the world: an online reference, v.6.0*. New York: American Museum of Natural History. Available at: https://amphibiansoftheworld.amnh.org/Museum-abbreviations. (Accessed January–April 2021).

Funch RR, **Harley RM**, **Funch LS. 2009.** Mapping and evaluation of the state of conservation of the vegetation in and surrounding the Chapada Diamantina National Park, NE Brazil. *Biota Neotropica* **9:** 21–30. Doi: 10.1590/S1676-06032009000200001.

Gonçalves GL, **de Freitas TRO. 2009.** Intraspecific variation and genetic differentiation of the collared tuco-tuco (*Ctenomys torquatus*) in southern Brazil. *Journal of Mammalogy* **90:** 1020–1031. Doi: 10.1644/07-MAMM-A-314.1.

Graboski R, **Filho GAP**, **da Silva AAA**, **Prudente ALDC**, **Zaher H. 2015.** A new species of *Amerotyphlops* from northeastern Brazil, with comments on distribution of related species. *Zootaxa* **3920:** 443–452. Doi: 10.11646/zootaxa.3920.3.3.

Graboski R, **Arredondo JC**, **Grazziotin FG**, **da Silva AAA**, **Prudente ALC**, **Rodrigues MT**, **Bonatto SL**, **Zaher H. 2018.** Molecular phylogeny and hemipenial diversity of South American species of *Amerotyphlops* (Typhlopidae, Scolecophidia). *Zoologica Scripta* **48:** 139–156. Doi: 10.1111/zsc.12334.

Grazziotin FG, **Monzel M**, **Echeverrigaray S**, **Bonatto SL. 2006.** Phylogeography of the *Bothrops jararaca* complex (Serpentes: Viperidae): past fragmentation and island colonization in the Brazilian Atlantic forest. *Molecular Ecology* **15:** 3969–3982. Doi: 10.1111/j.1365-294X.2006.03057.x.

Grazziotin FG, **Zaher H**, **Murphy RW**, **Scrocchi G**, **Benavides MA**, **Zhang YP**, **Bonatto SL. 2012.** Molecular phylogeny of the New World Dipsadidae (Serpentes: Colubroidea): a reappraisal. *Cladistics* **28:** 437–459. Doi: 10.1111/j.1096-0031.2012.00393.x.

Gross J, **Ligges U. 2015.** *Nortest: tests for normality. R package v.1.0-4*. Available at: https://CRAN.R-project.org/package=nortest. (Accessed April 2021).

Guedes TB, **Nogueira C**, **Marques OAV. 2014.** Diversity, natural history, and geographic distribution of snakes in the caatinga, northeastern Brazil. *Zootaxa* **3863:** 1–93. Doi: 10.11646/zootaxa.3863.1.1.

Hedges SB, **Marion AB**, **Lipp KM**, **Marin J**, **Vidal N. 2014.** A taxonomic framework for typhlopid snakes from the Caribbean and other regions (Reptilia, Squamata). *Caribbean Herpetology* **49:** 1–61. Doi: 10.31611/ch.49.

Hillis DM, **Mable BK**, **Moritz C. 1996.** Applications of molecular systematics. In: Hillis DM, Moritz C, Mable BK, eds. *Molecular systematics*. Sunderland: Sinauer Associates, 515–544. Doi: 10.2307/1447682.

Hüppop K. 2000. How do cave animals cope with the food scarcity in caves? In: Wilkens H, Culver D, Humphreys W, eds. *Subterranean ecosystems*. Amsterdam: Elsevier, 159–188.

Instituto Brasileiro de Geografia e Estatística. 2012. *Manual técnico da vegetação brasileira*. Rio de Janeiro: Instituto Brasileiro de Geografia e Estatística-IBGE.

Jan G. 1860. *Iconographie générale des ophidiens. 1. Livraison*. Paris: J.B. Bailière et Fils. https://doi.org/10.5962/bhl.title.4885

Jiménez A, **Savage JM. 1962.** A new blind snake (genus *Typhlops*) from Costa Rica. *Revista de Biologia Tropical* **10:** 199–203.

Katoh K, **Standley DM. 2013.** MAFFT multiple sequence alignment software version 7: improvements in performance and usability. *Molecular Biology and Evolution* **30:** 772–780. Doi: 10.1093/molbev/mst010.

Klauber LM. 1939. Three new worm snakes of the genus *Leptotyphlops*. *Transactions of the San Diego Society of Natural History* **9:** 59–65. https://doi.org/10.2307/1436008

Kearse M, **Moir R**, **Wilson A**, **Stones-Havas S**, **Cheung M**, **Sturrock S**, **Buxton S**, **Cooper A**, **Markowitz S**, **Duran C**, **Thierer T**, **Ashton B**, **Meintjes P**, **Drummond A. 2012.** Geneious Basic: an integrated and extendable desktop software platform for the organization and analysis of sequence data. *Bioinformatics* **28:** 1647–1649. Doi: 10.1093/bioinformatics/bts199.

Kuhn M. 2008. Building predictive models in R using the caret package. *Journal of Statistical Software* **28:** 1–26. Doi: 10.18637/jss.v028.i05.

Lanfear R, **Frandsen PB**, **Wright AM**, **Senfeld T**, **Calcott B. 2016.** PartitionFinder 2: new methods for selecting partitioned models of evolution for molecular and morphological phylogenetic analyses. *Molecular Biology and Evolution* **34:** 772–773. Doi: 10.1093/molbev/msw260.

Laver RJ, **Daza JD**, **Ellis RJ**, **Stanley EL**, **Bauer AM. 2021.** Underground down under: skull anatomy of the southern blind snake *Anilios australis* Gray, 1845 (Typhlopidae: Serpentes: Squamata). *The Anatomical Record* **304:** 2215–2242. Doi: 10.1002/ar.24696.

Lefébure T, **Douady CJ**, **Gouy M**, **Trontelj P**, **Briolay J**, **Gibert J. 2006.** Phylogeography of a subterranean amphipod reveals cryptic diversity and dynamic evolution in extreme environments: cryptic and dynamic evolution in subsurface. *Molecular Ecology* **15:** 1797–1806. Doi: 10.1111/j.1365-294X.2006.02888.x.

Linnaeus C. 1758. *Systema naturae per regna tria naturae: secundum classes, ordines, genera, species, cum characteribus, differentiis, synonymis, locis*. Stockholm: Salvius. Doi: 10.5962/bhl.title.542.

Lira I, **Martins A. 2021.** Digging into blindsnakes: morphology: description of the skull, lower jaw, and cervical vertebrae of two Amerotyphlops (Hedges *et al*., 2014) (Serpentes, Typhlopidae) with comments on the typhlopoidean skull morphological diversity. *The Anatomical Record* **2021:** 1–17. Doi: 10.1002/ar.24591.

Lirio EJ, **Peixoto AL**, **Siqueira MF. 2015.** Taxonomy, conservation, geographic and potential distribution of *Macrotorus* Perkins (Mollinedioideae, Monimiaceae), and a key to the Neotropical genera of Monimiaceae. *Phytotaxa* **234:** 201–214. Doi: 10.11646/phytotaxa.234.3.1.

List JC. 1966. *Comparative osteology of the snake families Typhlopidae and Leptotyphlopidae*. Urbana: University of Illinois Press. Doi: 10.5962/bhl.title.50341.

Maddock ST, **Nussbaum RA**, **Day JJ**, **Latta L**, **Miller M**, **Fisk DL**, **Wilkinson M**, **Rocha S**, **Gower DJ**, **Pfrender ME. 2020.** The roles of vicariance and isolation by distance in shaping biotic diversification across an ancient archipelago: evidence from a Seychelles caecilian amphibian. *BMC Evolutionary Biology* **20:** 110. Doi: 10.1186/s12862-020-01673-w.

Malard F, **Hervant F. 1999.** Oxygen supply and the adaptations of animals in groundwater. *Freshwater Biology* **41:** 1–30. Doi: 10.1046/j.1365-2427.1999.00379.x.

Marcy AE, **Hadly EA**, **Sherratt E**, **Garland K**, **Weisbecker V. 2016.** Getting a head in hard soils: convergent skull evolution and divergent allometric patterns explain shape variation in a highly diverse genus of pocket gophers (*Thomomys*). *BMC Evolutionary Biology* **16:** 207. Doi: 10.1186/s12862-016-0782-1.

Marin J, **Donnellan SC**, **Blair Hedges S**, **Doughty P**, **Hutchinson MN**, **Cruaud C**, **Vidal N. 2013a.** Tracing the history and biogeography of the Australian blindsnake radiation (J Masters, Ed.). *Journal of Biogeography* **40:** 928–937. https://doi.org/10.1111/jbi.12045

Marin J, **Donnellan SC**, **Hedges SB**, **Puillandre N**, **Aplin KP**, **Doughty P**, **Hutchinson MN**, **Couloux A**, **Vidal N. 2013b.** Hidden species diversity of Australian burrowing snakes (*Ramphotyphlops*): Australian Blindsnake Diversity. *Biological Journal of the Linnean Society* **110:** 427–441. https://doi.org/10.1111/bij.12132

Marques MCM, **Swaine MD**, **Liebsch D. 2011.** Diversity distribution and floristic differentiation of the coastal lowland vegetation: implications for the conservation of the Brazilian Atlantic Forest. *Biodiversity and Conservation* **20:** 153–168. Doi: 10.1007/s10531-010-9952-4.

Martins AR, **Silveira AL**, **Bruno SF. 2010.** New records of *Typhlops brongersmianus* (Serpentes, Typhlopidae) in southeastern Brazil. *Herpetology Notes* **3:** 247–248.

Massarini A, **Mizrahi D**, **Tiranti S**, **Toloza A**, **Luna F**, **Schleich CE. 2002.** Extensive chromosomal variation in *Ctenomys talarum talarum* from the Atlantic coast of Buenos Aires Province, Argentina (Rodentia: Octodontidae). *Mastozoologia Neotropical* **9:** 199–207.

Mattos JCF, **Vale M**, **Vecchi M**, **Alves M. 2009.** Abundance, distribution and conservation of the restinga antwren *Formicivora littoralis*. *Bird Conservation International* **19:** 392–400. Doi: 10.1017/S0959270909008697.

McDowell SB. 1967. Osteology of the Typhlopidae and Leptotyphlopidae: a critical review. *Copeia* **3:** 686–692. Doi: 10.2307/1442259.

McNab BK. 1966. The metabolism of fossorial rodents: a study of convergence. *Ecology* **47:** 712–733. Doi: 10.2307/1934259.

Medina RG, **Lira-Noriega A**, **Aráoz E**, **Ponssa ML. 2020.** Potential effects of climate change on a Neotropical frog genus: changes in the spatial diversity patterns of *Leptodactylus* (Anura, Leptodactylidae) and implications for their conservation. *Climatic Change* **161:** 535–553. Doi: 10.1007/s10584-020-02677-7.

Mocquard MF. 1905. Note préliminaire sur une collection de reptiles et de Batraciens offerte au Muséum par M. Maurice de Rothschild. *Bulletin du Muséum d'Histoire Naturelle, Paris* **11:** 285–288.

Montingelli GG, Gower DJ, Zaher H. 2002. Diversity and evolution of squamate hemipenes: an overview with particular reference to the origin and early history of snakes. In: Gower DJ, Zaher H, eds. *The Origin and Early Evolutionary History of Snakes*. Systematics Association Special Volume 90. Cambridge: Cambridge University Press, 351–388. https://doi.org/10.1017/9781108938891.022

Mulvaney A, **Castoe TA**, **Ashton KG**, **Krysko KL**, **Parkinson CL. 2005.** Evidence of population genetic structure within the Florida worm lizard, *Rhineura floridana* (Amphisbaenia: Rhineuridae). *Journal of Herpetology* **39:** 118–124. Doi: 10.1670/0022-1511(2005)039[0118:EOPGSW]2.0.CO;2.

Myers N, **Mittermeier RA**, **Mittermeier CG**, **da Fonseca GAB**, **Kent J. 2000.** Biodiversity hotspots for conservation priorities. *Nature* **403:** 853–858. Doi: 10.1038/35002501.

Nacif PGS, **Costa OV**, **Araújo M**, **Santos PS. 2009.** Geomorfodinâmica da Região do Complexo de Serras das Lontras. In: SAVE Brasil, IESB, BirdLife, eds. *Complexo de Serras das Lontras e Una, Bahia: Elementos naturais e aspectos de sua conservação*. São Paulo: SAVE Brasil, 9–14.

Nagy ZT, **Marion AB**, **Glaw F**, **Miralles A**, **Nopper J**, **Vences M**, **Hedges SB. 2015.** Molecular systematics and undescribed diversity of Madagascan scolecophidian snakes (Squamata: Serpentes). *Zootaxa* **4040:** 31–47. Doi: 10.11646/zootaxa.4040.1.3.

Nevo E. 1979. Adaptive convergence and divergence of subterranean mammals. *Annual Review of Ecology and Systematics* **1:** 269–308. Doi: 10.1146/annurev.es.10.110179.001413.

Nogueira CC, **Argôlo AJS**, **Arzamendia V**, **Azevedo JA**, **Barbo FE**, **Bérnils RS**, **Bolochio BE**, **Borges-Martins M**, **Brasil-Godinho M**, **Braz H**, **Buononato MA**, **Cisneros-Heredia DF**, **Colli GR**, **Costa HC**, **Franco FL**, **Giraudo A**, **Gonzalez RC**, **Guedes T**, **Hoogmoed MS**, **Marques OAV**, **Montingelli GG**, **Passos P**, **Prudente ALC**, **Rivas GA**, **Sanchez PM**, **Serrano FC**, **Silva NJ**, **Strüssmann C**, **Vieira-Alencar JPS**, **Zaher H**, **Sawaya RJ**, **Martins M. 2019.** Atlas of Brazilian snakes: verified point-locality maps to mitigate the Wallacean shortfall in a megadiverse snake fauna. *South American Journal of Herpetology* **14:** 1–274. Doi: 10.2994/SAJH-D-19-00120.1.

O'Connell KA, **Prates I**, **Scheinberg LA**, **Mulder KP**, **Bell RC. 2021.** Speciation and secondary contact in a fossorial island endemic, the São Tomé caecilian. *Molecular Ecology* **30:** 2859–2871. Doi: 10.1111/mec.15928.

Olson DM, **Dinerstein E**, **Wikramanayake ED**, **Burgess ND**, **Powell GVN**, **Underwood EC**, **D'amico JA**, **Itoua I**, **Strand HE**, **Morrison JC**, **Loucks CJ**, **Allnutt TF**, **Ricketts TH**, **Kura Y**, **Lamoreux JF**, **Wettengel WW**, **Hedao P**, **Kassem KR. 2001.** Terrestrial ecoregions of the world: a new map of life on earth. *BioScience* **51:** 933–938. Doi: 10.1641/0006-3568(2001)051[0933:TEOTWA]2.0.CO;2.

Palci A, **Lee MSY**, **Hutchinson MN. 2016.** Patterns of postnatal ontogeny of the skull and lower jaw of snakes as revealed by micro-CT scan data and three-dimensional geometric morphometrics. *Journal of Anatomy* **229:** 723–754. Doi: 10.1111/joa.12509.

Paradis E, **Schliep K. 2019.** Ape 5.0: an environment for modern phylogenetics and evolutionary analyses in R. *Bioinformatics* **35:** 526–528. Doi: 10.1093/bioinformatics/bty633.

Parham JF, **Papenfuss TJ. 2009.** High genetic diversity among fossorial lizard populations (*Anniella pulchra*) in a rapidly developing landscape (central California). *Conservation Genetics* **10:** 169–176. Doi: 10.1007/s10592-008-9544-y.

Peel MC, **Finlayson BL**, **McMahon TA. 2007.** Updated world map of the Köppen–Geiger climate classification. *Hydrology and Earth System Sciences* **11:** 1633–1644. Doi: 10.5194/hess-11-1633-2007.

Pellegrino KCM, **Rodrigues MT**, **Waite AN**, **Morando M**, **Yassuda YY**, **Sites JW. 2005.** Phylogeography and species limits in the *Gymnodactylus darwinii* complex (Gekkonidae, Squamata): genetic structure coincides with river systems in the Brazilian atlantic forest. *Biological Journal of the Linnean Society* **85:** 13–26. Doi: 10.1111/j.1095-8312.2005.00472.x.

Peters WCH. 1858. Vier neue amerikanische Schlangen aus der Familie der Typhlopinen vor und machte darüber einige vorläufige. *Mittheilungen. Monatsberichte der Königlichen Preussische Akademie des Wissenschaften zu Berlin* **1857:** 402–403.

Peters JA, **Orejas-Miranda BR. 1970.** Notes on the hemipenis of several taxa in the family Leptotyphlopidae. *Herpetologica* **26:** 320–324.

Pinto RR, **Martins AR**, **Curcio F**, **Ramos LO. 2015.** Osteology and cartilaginous elements of *Trilepida salgueiroi* (Amaral, 1954) (Scolecophidia: Leptotyphlopidae). *The Anatomical Record* **298:** 1722–1747. Doi: 10.1002/ar.23191.

Pyron RA, **Wallach V. 2014.** Systematics of the blindsnakes (Serpentes: Scolecophidia: Typhlopoidea) based on molecular and morphological evidence. *Zootaxa* **3829:** 1–81. Doi: 10.11646/zootaxa.3829.1.1.

de Queiroz K. 2005. A unified concept of species and its consequences for the future of taxonomy. *Proceedings of the California Academy of Science* **56:** 196–215.

R Core Team. 2017. *R: a language and environment for statistical computing*. Vienna: R Foundation for Statistical Computing. Available at: https://www.r-project.org. (Accessed January 2021).

Recoder RS, **Junior MT**, **Cassimiro J**, **Camacho A**, **Rodrigues MT. 2010.** A new species of *Dendrophryniscus* (Amphibia, Anura, Bufonidae) from the Atlantic rainforest of southern Bahia, Brazil. *Zootaxa* **2642:** 36–44. Doi: 10.11646/zootaxa.2642.1.3.

Reig OA, **Busch C**, **Ortells MO**, **Contreras JR. 1990.** An overview of evolution, systematics, population biology, cytogenetics, molecular biology and speciation in *Ctenomys*. *Progress in Clinical and Biological Research* **335:** 71–96.

Reis JRM, **Fontoura T. 2009.** Diversidade de bromélias epífitas na Reserva Particular do Patrimônio Natural Serra do Teimoso–Jussari, BA. *Biota Neotropica* **9:** 73–79. Doi: 10.1590/S1676-06032009000100009.

Ribeiro MC, **Metzger JP**, **Martensen AC**, **Ponzoni FJ**, **Hirota MM. 2009.** The Brazilian Atlantic forest: how much is left, and how is the remaining forest distributed? Implications for conservation. *Biological Conservation* **142:** 1141–1153. Doi: 10.1016/j.biocon.2009.02.021.

Richmond ND. 1955. The blind snakes (*Typhlops*) of Bimini, Bahama Islands, British West Indies, with description of a new species. *American Museum Novitates* **1734:** 1–7.

Richmond ND. 1965. A new species of blind snake, *Typhlops*, from Trinidad. *Proceedings of the Biological Society of Washington* **78:** 121–124.

Richmond ND. 1966. The Blind Snakes, *Typhlops*, of Guadeloupe and Dominica with the description of a new species. *Herpetologica* **22:** 129–132.

Riesch R, **Tobler M**, **Plath M. 2015.** *Extremophile fishes: ecology, evolution, and physiology of teleosts in extreme environments*. Heidelberg: Springer. Doi: 10.1007/978-3-319-13362-1.

Rizzini CT. 1997. *Tratado de fitogeografia do Brasil: aspectos ecológicos, sociológicos e florísticos*. Rio de Janeiro: Ambito Cultural.

Roberto IJ, **Ávila RW**, **Melgarejo AR. 2015.** Répteis (Testudines, Squamata, Crocodylia) da Reserva Biológica de Pedra Talhada. In: Studer A, Nusbaumer L, Spichiger R, eds. Biodiversidade da Reserva Biológica de Pedra Talhada (Alagoas, Pernambuco - Brasil). *Boissiera* **68:** 357–375.

Roberto IJ, **de Oliveira CR**, **de Araújo Filho JA**, **de Oliveira HF**, **Ávila RW. 2017.** The herpetofauna of the Serra do Urubu mountain range: a key biodiversity area for conservation in the Brazilian Atlantic forest. *Papéis Avulsos de Zoologia* **57:** 347–373. Doi: 10.11606/0031-1049.2017.57.27.

Rocha CFD, **Sluys MV. 2007.** Herpetofauna de restingas. In: Nascimento LB, Oliveira ME, eds. *Herpetologia no Brasil II*. Belo Horizonte: Sociedade Brasileira de Herpetologia, 354.

Rocha C, **Sluys M**, **Bergallo HG**, **Alves MAS. 2005.** Endemic and threatened tetrapods in the restingas of the biodiversity corridors of Serra do Mar and of the central da Mata Atlântica in eastern Brazil. *Brazilian Journal of Biology* **65:** 159–168. Doi: 10.1590/S1519-69842005000100019.

Rocha C, **Bergallo H**, **Sluys M**, **Alves M**, **Jamel C. 2007.** The remnants of Restinga habitats in the Brazilian Atlantic forest of Rio de Janeiro state, Brazil: habitat loss and risk of disappearance. *Brazilian Journal of Biology* **67:** 263–273. Doi: 10.1590/S1519-69842007000200011.

Rodrigues MT. 1991. Herpetofauna das dunas interiores do Rio São Francisco: Bahia: Brasil. IV. Uma nova espécie de *Typhlops* (Ophidia, Typhlopidae). *Papéis Avulsos de Zoologia* **37:** 343–346.

Rodrigues MT, **Juncá FA. 2002.** Herpetofauna of the quaternary sand dunes of the middle Rio São Francisco: Bahia: Brazil. VII.: *Typhlops amoipira* sp. nov., a possible relative of *Typhlops yonenagae* (Serpentes, Typhlopidae). *Papéis Avulsos de Zoologia* **42:** 325–333. Doi: 10.1590/S0031-10492002001300001.

Rodrigues MT, **Dixo M**, **Pavan D**, **Verdade VK. 2002.** A new species of *Leposoma* (Squamata, Gymnophthalmidae) from the remnant Atlantic forests of the state of Bahia, Brazil. *Papéis Avulsos de Zoologia* **42:** 335–350. Doi: 10.1590/S0031-10492002001400001.

Rodrigues MT, **Teixeira Jr. M**, **Recoder RS**, **Dal Vechio F**, **Damasceno R**, **Pellegrino KCM. 2013.** A new species of *Leposoma* (Squamata: Gymnophthalmidae) with four fingers from the Atlantic Forest central corridor in Bahia, Brazil. *Zootaxa* **3635:** 459–475. Doi: 10.11646/zootaxa.3635.4.7.

Rossman CE. 1980. Ontogenetic changes in skull proportions of the diamondback water snake, *Nerodia rhombifera*. *Herpetologica* **36:** 42–46.

Roux J. 1926. Notes d'erpétologie Sud-Américaine. 2. Sur une nouvelle espèce de *Typhlops T. lehneri* du Vénézuela. *Revue Suisse de Zoologie* **33:** 291–299.

Roze JA. 1956. Ofidios coleccionados por la expedición Franco Venezolana al alto Orinoco 1951–1952. *Boletín del Museo de Ciencias Naturales* **1:** 179–195.

Sabaj MH. 2019. *Standard Symbolic codes for institutional resource collections in herpetology and ichthyology: an online reference, v.7.1 (21 March 2019)*. Available at: https://asih.org/. (Accessed January 2021).

Sackett JT. 1940. Preliminary report on results of the West Indies-Guatemala expedition of 1940 for the Academy of Natural Sciences of Philadelphia. Part I. A new blind snake of the genus *Typhlops*. *Notulae Naturae of the Academy of Natural Sciences of Philadelphia* **48:** 1–2.

Saiter FZ, **Brown JL**, **Thomas WW**, **de Oliveira-Filho AT**, **Carnaval AC. 2016.** Environmental correlates of floristic regions and plant turnover in the Atlantic forest hotspot. *Journal of Biogeography* **43:** 2322–2331. Doi: 10.1111/jbi.12774.

Salvin O. 1860. On the reptiles of Guatemala. *Proceedings of the Academy of Natural Sciences of Philadelphia* **1860:** 451–461.

Santana GG, **Vieira WLS**, **Pereira-Filho GA**, **Delfim FR**, **Lima YC**, **Vieira KS. 2008.** Herpetofauna em um fragmento de Floresta Atlântica no Estado da Paraíba, Região Nordeste do Brasil. *Biotemas* **21:** 75–84. Doi: 10.5007/2175-7925.2008v21n1p75.

Santos VDJ. 2013. *Restingas do estado da Bahia: riqueza, diversidade e estrutura*. Unpublished DPhil, Universidade Federal Rural de Pernambuco.

Savage JM. 1950. Two new blind snakes (genus *Typhlops*) from the Philippine Islands. *Proceedings of the California Zoological Club* **1:** 49–54.

Scanferla A, **Bhullar BAS. 2014.** Postnatal development of the skull of *Dinilysia patagonica* (Squamata-Stem Serpentes). *The Anatomical Record* **297:** 560–573. https://doi.org/10.1002/ar.22862

Scarano FR. 2006. Plant community structure and function in a swamp forest within the Atlantic rain forest complex: a synthesis. *Rodriguésia* **57:** 491–502. Doi: 10.1590/2175-7860200657308.

Schmidt KP. 1936. New amphibians and reptiles from Honduras in the Museum of Comparative Zoology. *Proceedings of the Biological Society of Washington* **49:** 43–50.

Silva LA, **Satyamurty P. 2006.** The role of the upper tropospheric cyclonic systems in the northeast of Brazil rain inhibition. *Proceedings of the 8th International Conference on Southern Hemisphere Meteorology and Oceanography*. Foz do Iguaçú, Brazil: American Meteorological Society, Boston, 2027–2031.

Silva W, **Metzger J**, **Simões S**, **Simonetti C. 2007.** Relief influence on the spatial distribution of the Atlantic Forest cover on the Ibiúna Plateau, SP. *Brazilian Journal of Biology* **67:** 403–411. Doi: 10.1590/S1519-69842007000300004.

Silveira LF, **Develey PF**, **Pacheco JF**, **Whitney BM. 2005.** Avifauna of the Serra das Lontras–Javi montane complex, Bahia, Brazil. *Cotinga* **24:** 45–54.

SOS Mata Atlântica, Instituto Nacional de Pesquisas Espaciais. 2000. *Atlas dos Remanescentes Florestais e Ecossistemas Associados no Domínio da Mata Atlântica*. São Paulo: Fundação SOS Mata Atlântica.

Stamatakis A. 2014. RAxML version 8: a tool for phylogenetic analysis and post-analysis of large phylogenies. *Bioinformatics* **30:** 1312–1313. Doi: 10.1093/bioinformatics/btu033.

Stayton CT. 2005. Morphological evolution of the lizard skull: a geometric morphometrics survey. *Journal of Morphology* **263:** 47–59. Doi: 10.1002/jmor.10288.

Steinberg EK, **Patton JL**, **Lacey E. 2000.** Genetic structure and the geography of speciation in subterranean rodents: opportunities and constraints for evolutionary diversification. In: Lacey EA, Patton JL, Cameron GN, eds. *Life underground: the biology of subterranean rodents*. Chicago: University of Chicago Press, 301–331.

Struck TH, **Cerca J. 2019.** Cryptic species and their evolutionary significance. In: *Encyclopedia of life sciences*. Chichester: John Wiley & Sons Ltd, 1–9.

Struck TH, **Feder JL**, **Bendiksby M**, **Birkeland S**, **Cerca J**, **Gusarov VI**, **Kistenich S**, **Larsson KH**, **Liow LH**, **Nowak MD**, **Stedje B**, **Bachmann L**, **Dimitrov D. 2018.** Finding evolutionary processes hidden in cryptic species. *Trends in Ecology & Evolution* **33:** 153–163. Doi: 10.1016/j.tree.2017.11.007.

Swift HF, **Gómez Daglio L**, **Dawson MN. 2016.** Three routes to crypsis: stasis, convergence, and parallelism in the *Mastigias* species complex (Scyphozoa, Rhizostomeae). *Molecular Phylogenetics and Evolution* **99:** 103–115. Doi: 10.1016/j.ympev.2016.02.013.

Telles FBS, **Menezes VA**, **Maia-Carneiro T**, **Dorigo TA**, **Winck GR**, **Rocha CFD. 2012.** Anurans from the 'restinga' of Parque Natural Municipal de Grumari, state of Rio de Janeiro, southeastern Brazil. *Check List* **8:** 1267–1273. Doi: 10.15560/8.6.1267.

Thomas R. 1966. A reassessment of the Virgin Islands *Typhlops* with the description of two new subspecies. *Revista de Biologia Tropical* **13:** 187–201.

Thomas R. 1974. A new species of lesser Antilles Typhlops (Serpentes: Typhlopidae). *Occasional Papers of the Museum of Zoology of Louisiana State University* **46:** 1–5. Doi: 10.31390/opmns.046.

Thomas R, **Hedges SB. 2007.** Eleven new species of snakes of the genus *Typhlops* (Serpentes: Typhlopidae) from Hispaniola and Cuba. *Zootaxa* **1400:** 1–26. Doi: 10.11646/zootaxa.1400.1.1.

Thomas WMW, **Carvalho AMV**, **Amorim AMA**, **Garrison J**, **Arbela A. 1998.** Plant endemism in two forests in southern Bahia, Brazil. *Biodiversity & Conservation* **7:** 311–322. Doi: 10.1023/A:1008825627656.

Thomé MTC, **Zamudio KR**, **Giovanelli JGR**, **Haddad CFB**, **Baldissera FA**, **Alexandrino J. 2010.** Phylogeography of endemic toads and post-Pliocene persistence of the Brazilian Atlantic Forest. *Molecular Phylogenetics and Evolution* **55:** 1018–1031. Doi: 10.1016/j.ympev.2010.02.003.

Tobler M, **Kelley JL**, **Plath M**, **Riesch R. 2018.** Extreme environments and the origins of biodiversity: adaptation and speciation in sulphide spring fishes. *Molecular Ecology* **27:** 843–859. Doi: 10.1111/mec.14497.

Townsend JH, **Wilson LD**, **Ketzler LP**, **Luque-Montes IR. 2008.** The largest blindsnake in Mesoamerica: a new species of *Typhlops* (Squamata: Typhlopidae) from an isolated karstic mountain in Honduras. *Zootaxa* **1932:** 18–26. Doi: 10.11646/zootaxa.1932.1.2.

Vanables WN, **Ripley BD. 2002.** *Modern applied statistics with S*. New York: Springer. Doi: 10.1007/978-0-387-21706-2.

Van-Silva W, **Guedes AG**, **de Azevedo-Silva PL**, **Gontijo FF**, **Barbosa RS**, **Aloísio GR**, **de Oliveira FCG. 2007.** Herpetofauna, Espora hydroelectric power plant, state of Goiás, Brazil. *Check List* **3:** 338–345. Doi: 10.15560/3.4.338.

Vanzolini PE. 1972. *Typhlops brongersmai* spec. nov. from the Coast of Bahia, Brasil (Serpentes, Typhlopidae). *Zoologische Mededelingen Leiden* **47:** 27–29.

Vanzolini PE. 1976. *Typhlops brongersmianus*, a new name for *Typhlops brongersmai* Vanzolini, 1972, Preoccupied (Serpentes, Typhlopidae). *Papéis Avulsos de Zoologia* **24:** 247.

Veloso HP, **Rangel Filho ALR**, **Lima JCA. 1991.** *Classificação da vegetação brasileira, adaptada a um sistema universal*. Rio de Janeiro: Ministério da Economia, Fazenda e Planejamento, Fundação Instituto Brasileiro de Geografia e Estatística, Diretoria de Geociências, Departamento de Recursos Naturais e Estudos Ambientais.

Vidal N, **Marin J**, **Morini M**, **Donnellan S**, **Branch WR**, **Thomas R**, **Vences M**, **Wynn A**, **Cruaud C**, **Hedges SB. 2010.** Blindsnake evolutionary tree reveals long history on Gondwana. *Biology Letters* **6:** 558–561. Doi: 10.1098/rsbl.2010.0220.

Vu VQ. 2011. *Ggbiplot: a ggplot2 based biplot. R package.* Available at: https://github.com/vqv/ggbiplot (Accessed April 2021).

Wallach V. 1998. *The visceral anatomy of Blindsnakes and Wormsnakes and its Systematic Implications (Serpentes: Anomalepididae: Typhlopidae: Leptotyphlopidae)*. Unpublished thesis, Northeastern University, Boston, MA.

Wallach V, **Williams KL**, **Boundy J. 2014.** *Snakes of the world: a catalogue of living and extinct species*. Boca Raton: CRC Press. Doi: 10.1201/b16901.

Wharton DA. 2002. *Life at the limits: organisms in extreme environments*. Cambridge: Cambridge University Press. Doi: 10.1017/CBO9780511541568.

Wickham H. 2016. *Ggplot2: elegant graphics for data analysis*. New York: Springer-Verlag. Doi: 10.1007/978-3-319-24277-4_9.

Winker K. 2005. Sibling species were first recognized by William Derham (1718). *The Auk* **122:** 706–707. Doi: 10.1093/auk/122.2.706.

Zaher H. 1999. Hemipenial morphology of the South American Xenodontine snakes, with a proposal for a monophyletic Xenodontinae and a reappraisal of colubroid hemipenes. *Bulletin of the American Museum of Natural History* **240:** 1–172.

Zaher H, **Prudente ALC. 2003.** Hemipenes of *Siphlophis* (Serpentes, Xenodontinae) and techniques of hemipenial preparation in snakes: a response to Dowling. *Herpetological Review* **34:** 302–307.

Zaher H, **Grazziotin FG**, **Cadle JE**, **Murphy RW**, **de Moura-Leite JC**, **Bonatto SL. 2009.** Molecular phylogeny of advanced snakes (Serpentes, Caenophidia) with an emphasis on South American Xenodontines: a revised classification and descriptions of new taxa. *Papéis Avulsos de Zoologia* **49:** 115–153. Doi: 10.1590/S0031-10492009001100001.

SUPPORTING INFORMATION

Additional Supporting Information may be found in the online version of this article at the publisher's web-site.

Appendix S1. Concatenated alignment used in this study to perform molecular analysis.
Appendix S2. List of specimens examined (pholidosis). Information on the museum in which they are stored, voucher and locality is given. (*) Hemipenis from specimens examined and (#) high resolution x-ray computed tomography (HRXCT) of cranial osteology examined.
Appendix S3. List of specimens examined (morphometrics). Information on the museum in which they are stored, the voucher and the locality is given.
Appendix S4. Boxplot of 36 characters for nine OTUs (separated by sex when sexual dimorphism is significant). *Continuous characters* – Fig. a, total length (TTL); Fig. b, snout–vent length (SVL); Fig. c, tail length (TL); Fig. d, head width at the level of the eyes (HWE); Fig. e, standard maximum width of the dorsal portion of the rostral to the internasal (RW1); Fig. f, standard length of the rostral from the internasal sutures (RL1); Fig. g, internarial distance (IN); Fig. h, midbody diameter (MBD); Fig. i, naris–eye distance (NE); Fig. j, mid-tail width (MTW); Fig. k, head radius (HR); Fig. l, eye diameter (ED); Fig. m, interorbital distance (INORB); Fig. n, width of the rostral on the apex of the snout (RW2); Fig. o, width of the rostral at the labial border (RW3); *Ratios* – Fig. p, ratio between tail length and snout-vent length (TL/SVL); Fig. q, ratio between midbody diameter and snout–vent length minus head radius (MBD/(SVL-HR)); Fig. r, ratio between head width at the level of the eyes and head radius (HWE/HR); Fig. s, ratio between rostral width and rostral length (RW1/RL1); Fig. t, ratio between interorbital distance and head width (INORB/HWE); Fig. u, ratio between the width of the rostral on the apex of the snout and rostral length (RW2/RL1); Fig. v, ratio between rostral length and head width (RL1/HWE); Fig. w, ratio between eye diameter and head width (ED/HWE); Fig. x, ratio between the width of the rostral at the labial border and rostral length (RW3/RL1); Fig. y, ratio between naris–eye distance and head radius (NE/HR); Fig. z, ratio between mid-tail width and snout–vent length (MTW/SVL); Fig. aa, ratio between mid-tail width and tail length (MTW/TL); Fig. ab, robustness of the head (HR/(SVL-HR)); Fig. ac, ratio between width of the rostral on the apex of the snout and rostral width (RW2/RW1); *Discrete characters* – Fig. ad, number of ventral scales (V); Fig. ae, number of dorsal scales (D); Fig. af, number of subcaudal scales (SbC); Fig. ag, number of scale rows around the anterior body (ROW-a); Fig. ah, number of scale rows around the midbody (ROW-m); Fig. ai, number of scale rows around the posterior body (ROW-p); and Fig. aj, number of dorso-cloacal scales (DC).
Figure S1. Maximum likelihood tree generated by RAxML. The numbers on the branch represent bootstrap values > 75%.
Figure S2. Results of principal component analysis (PCA) using the raw dataset based on 36 characters for nine OTUs. A, Group 1 (GR1). B, PCA of Group 2 (GR2). Species are colour-coded according to OTUs (see Key-colour OTUs, on the bottom).
Figure S3. Holotype of *Amerotyphlops caetanoi* (MZUSP S-023380). Specimen in dorsal (A) and ventral (B) views. TTL = 176 mm.
Figure S4. Holotype of *Amerotyphlops montanum* (MZUSP 20065). Specimen in dorsal (A) and ventral (B) views. TTL = 216 mm.
Figure S5. Holotype of *Amerotyphlops martis* (MNRJ 18744). Specimen in dorsal (A) and ventral (B) views. TTL = 157 mm.

Figure S6. Paratypes of *Amerotyphlops martis*: (MNRJ 18743) specimen in dorsal (A) and ventral (B) views, TTL = 170 mm. (MNRJ 18745) specimen in dorsal (C) and ventral (D) views, TTL = 130 mm. (MNRJ 18747) specimen in dorsal (E) and ventral (F) views, TTL = 145 mm.
Figure S7. Holotype of *Amerotyphlops illusorium* (MZUSP 18787). Specimen in dorsal (A) and ventral (B) views. TTL = 229 mm
Figure S8. Paratypes of *Amerotyphlops illusorium*: (MNRJ 19613) specimen in dorsal (A) and ventral (B) views, TTL = 207 mm. (MNRJ 19614) specimen in dorsal (C) and ventral (D) views, TTL = 151 mm.
Table S1. Detailed distribution of South American species of *Amerotyphlops*.
Table S2. List of taxa sequenced using Sanger methods used in this study. Information on the museum in which they are stored, the voucher and the locality is given.
Table S3. List of taxa and GenBank accession number of specimens used Sanger sequencing methods for this study. Codes in bold represent the sequences generated in this study.
Table S4. List of 50 taxonomic characters collected in this study for South American species of *Amerotyphlops*.
Table S5. Variation of osteological measures. Values displayed in the table are in mm. Abbreviations are as following: SL, skull length; SW, skull width; VPPL, length of the ventral pterygoid process of the palatine; and PFD, palatine foramen diameter.
Table S6. Best-fit models for 20 data partitions as determined by PARTITIONFINDER analyses using the AIC optimality criterion to run RAxML.
Table S7. Patristic distance among species of *Cubatyphlops*.
Table S8. Patristic distance among species of *Antillotyphlops*.
Table S9. Patristic distance among species of *Typhlops*.
Table S10. Patristic distance among species of *Amerotyphlops*.
Table S11. Results of MANOVA non-parametric analysis (MANOVA-NP) using the simulated dataset based on 36 characters for nine OTUs.